
PACING OPINION POLARIZATION VIA GRAPH REINFORCEMENT LEARNING *

Mingkai Liao
CSSE, Shenzhen University
Shenzhen, China
{13542830854@163.com}

ABSTRACT

Opinion polarization in online social networks poses a critical challenge to social cohesion and democratic processes. Recent work formulates polarization moderation as algorithmic intervention problems under opinion dynamics models, most notably the Friedkin–Johnsen (FJ) model. However, existing approaches are largely tailored to specific linear settings and rely on closed-form steady-state analysis, limiting their scalability, adaptability, and applicability to cost-aware, nonlinear, or topology-altering interventions.

In this paper, we propose **PACIFIER**, a graph reinforcement learning framework for sequential polarization moderation via network interventions. PACIFIER reformulates the canonical **MODERATEINTERNAL** (MI) and **MODERATEEXPRESSED** (ME) problems as sequential decision-making tasks, enabling adaptive policies without repeated recomputation of steady-state solutions. The framework is objective-agnostic and naturally extends to a broad class of FJ-consistent settings, including budget-aware interventions, continuous internal opinions, biased-assimilation dynamics, and node removal.

We introduce a temporal-aware node marking mechanism to encode intervention history under fixed topology, together with polarization-aware global features that correlate with polarization regimes while avoiding expensive steady-state recomputation during planning. Extensive experiments on 15 real-world Twitter follow and retweet networks (up to 155,599 nodes) demonstrate strong and consistent performance. In expressive-opinion moderation tasks (ME and ME-cost), PACIFIER-RL achieves a 100% win rate against the strongest non-learning baselines, yielding average improvements of 15%–40% in AUC. Under cost-aware MI settings, both RL and greedy variants consistently dominate all baselines with nearly 40% average gains. Even under nonlinear biased-assimilation dynamics and topology-changing node removal interventions, PACIFIER-RL maintains robust superiority, while in linear MI settings it performs competitively with near-optimal analytical methods.

These results establish graph reinforcement learning as a unified, scalable, and robust paradigm for pacing and moderating opinion polarization across diverse dynamical regimes and intervention mechanisms.

Keywords Opinion Polarization · Graph Reinforcement Learning · Network Intervention · Opinion Dynamics · Social Networks

1 Introduction

Opinion polarization has emerged as one of the most pressing challenges in contemporary online social networks, with far-reaching consequences for democratic discourse, public health, and societal stability. Extensive empirical evidence documents the formation of “echo chambers” and “filter bubbles,” in which individuals become increasingly insulated within homogeneous information environments that reinforce pre-existing beliefs while marginalizing opposing viewpoints. Such polarization is not merely a theoretical concern; it has been linked to political fragmentation,

**Citation: Authors. Title. Pages.... DOI:000000/11111.*

large-scale misinformation diffusion, and adverse public health outcomes during societal crises. Addressing opinion polarization therefore calls for principled, scalable, and adaptable computational intervention frameworks capable of operating on large and heterogeneous social networks.

A foundational line of work on algorithmic polarization moderation was established by Matakos et al. [1], who formalized two canonical intervention problems under the Friedkin–Johnsen (FJ) opinion dynamics model [2]: `MODERATEINTERNAL` (MI) and `MODERATEEXPRESSED` (ME). These problems capture two complementary intervention paradigms: modifying individuals’ internal (stubborn) opinions and directly regulating their expressed opinions. Leveraging the linear-algebraic structure of the FJ model, prior work proposed efficient heuristics such as Binary Orthogonal Matching Pursuit (BOMP) for MI and greedy selection strategies for ME. While analytically elegant and effective in strictly linear settings, these approaches are tightly coupled to model-specific assumptions and steady-state closed-form analysis. Consequently, they are difficult to generalize to cost-aware interventions, nonlinear opinion dynamics, or topology-altering mechanisms such as node removal.

More broadly, polarization moderation is computationally challenging and often NP-hard [3], limiting the scalability of classical optimization-based approaches. Even polynomial-time methods such as BOMP incur $O(n^2)$ complexity, which becomes prohibitive on large real-world graphs. Moreover, once nonlinear opinion dynamics or heterogeneous intervention constraints are introduced, steady-state closed-form analysis may no longer exist or may become analytically intractable. These limitations motivate the search for a unified framework that (i) scales to large networks, (ii) adapts across intervention paradigms, and (iii) remains robust under structurally consistent nonlinear extensions of the FJ model.

The primary contribution of this work is the introduction of **PACIFIER**, a graph reinforcement learning framework for sequential polarization moderation. We reformulate the MI and ME problems as sequential decision-making tasks over networked opinion dynamics, enabling the learning of adaptive intervention policies without relying on repeated steady-state recomputation or handcrafted heuristics. Unlike prior analytical approaches, PACIFIER is objective-agnostic: the agent optimizes any polarization-related objective specified through its reward function. Within this unified paradigm, we demonstrate that PACIFIER naturally extends beyond the original linear MI/ME settings to several practically relevant regimes, including cost-aware intervention, continuous-valued internal opinions, biased-assimilation nonlinear dynamics, and topology-altering node removal.

Empirically, PACIFIER exhibits strong and consistent performance across diverse tasks and datasets. On 15 real-world Twitter follow and retweet networks (up to 155,599 nodes), PACIFIER-RL achieves a 100% win rate over the strongest non-learning baselines in expressive-opinion moderation (ME and ME-cost), yielding substantial reductions in accumulated polarization. Under cost-aware MI settings, both the RL and greedy variants consistently outperform all classical baselines. Even in nonlinear and topology-changing regimes—where traditional analytical methods lose their structural advantages—PACIFIER-RL maintains robust superiority. At the same time, in strictly linear MI settings where near-optimal analytical solvers exist, PACIFIER remains competitive, demonstrating that learning-based policies do not sacrifice performance in regimes where closed-form solutions are strong.

Inspired by the success of graph reinforcement learning in network intervention problems such as network dismantling [4], PACIFIER bridges structural graph optimization and opinion dynamics by jointly modeling network topology, opinion evolution, and intervention history. Adopting an inductive training paradigm, the agent is trained on small synthetic graphs and directly generalizes to large-scale real networks, enabling scalable deployment across heterogeneous social systems.

Our second major contribution addresses two representation challenges unique to polarization moderation under topology-preserving interventions.

First, when the network structure $G = (V, E)$ remains fixed and interventions only modify node or edge attributes, different intervention histories may produce nearly indistinguishable graph observations. This history-induced ambiguity leads to state aliasing and unstable credit assignment in graph reinforcement learning. We formalize topology-preserving interventions in Definition 4.1 and introduce a temporal-aware node marking mechanism that explicitly encodes intervention history into node features, ensuring that the encoder distinguishes otherwise identical states.

Second, we incorporate polarization-aware global signals into the state encoder by combining node-level opinion features with graph-level structural cues. These features correlate with polarization regimes and guide value estimation without requiring expensive steady-state recomputation during planning.

Together, these representation mechanisms enable PACIFIER to operate effectively across topology-preserving and topology-altering regimes, establishing it as a unified, scalable, and extensible framework for moderating opinion polarization under diverse dynamical and intervention settings.

1.1 Contributions

The main contributions of this work are summarized as follows:

- **PACIFIER: a unified graph reinforcement learning framework for polarization moderation.** We propose **PACIFIER**, a graph reinforcement learning framework that reformulates the canonical MODERATEINTERNAL (MI) and MODERATEEXPRESSED (ME) problems as sequential decision-making tasks over networked opinion dynamics. Unlike prior analytical or heuristic methods tied to steady-state closed-form analysis, PACIFIER learns adaptive intervention policies directly through interaction, enabling scalable optimization on large social networks without repeated recomputation of equilibrium solutions.
- **Generalization across intervention paradigms and FJ-consistent dynamics.** Within a single objective-agnostic learning framework, PACIFIER extends beyond the original linear MI/ME settings to multiple practically relevant regimes, including cost-aware interventions, continuous-valued internal opinions, homogeneous nonlinear biased-assimilation dynamics, and topology-altering node removal. This establishes a unified moderation paradigm that remains robust under structurally consistent extensions of the Friedkin–Johnsen model.
- **Representation mechanisms for topology-preserving and polarization-aware learning.** We address two key challenges in graph reinforcement learning for polarization moderation: (i) a temporal-aware node marking mechanism that resolves history-induced state aliasing under topology-preserving interventions, and (ii) polarization-aware global feature integration that improves value estimation without requiring expensive steady-state recomputation. These mechanisms enable stable credit assignment and effective policy learning across diverse intervention regimes.
- **Extensive empirical validation on large-scale real networks.** We evaluate PACIFIER on 15 real-world Twitter follow and retweet networks with sizes up to 155,599 nodes across multiple intervention tasks and dynamical regimes. PACIFIER-RL achieves a 100% win rate over the strongest non-learning baselines in expressive-opinion moderation (ME and ME-cost), yields nearly 40% average improvement in cost-aware MI settings, and maintains strong superiority under nonlinear and topology-changing interventions. At the same time, PACIFIER remains competitive with near-optimal analytical solvers in strictly linear MI settings, demonstrating both robustness and adaptability across regimes.

1.2 Paper Organization

The remainder of this paper is organized as follows. Section 2 reviews related work on opinion polarization, moderation algorithms, and graph reinforcement learning. Section 3 formalizes the MODERATEINTERNAL and MODERATEEXPRESSED problems under the Friedkin–Johnsen model and introduces FJ-consistent nonlinear and extended intervention settings. Section 4 presents the PACIFIER framework, including the reinforcement learning formulation, the temporal-aware node marking mechanism, and the polarization-aware feature design. Section 5 reports experimental results on synthetic and real-world networks across base and extended regimes. Finally, Section 6 concludes the paper and discusses future research directions.

2 Related Work

Despite substantial progress in both opinion-dynamics modeling and network intervention, existing approaches remain divided between model-specific analytical optimization and learning-based structural intervention, with limited integration across the two paradigms. Our work lies at the intersection of three research directions: (i) opinion polarization modeling and algorithmic moderation under opinion dynamics, (ii) traditional network intervention and key-player identification, and (iii) graph reinforcement learning for sequential decision making on networks. We briefly review each stream and clarify how PACIFIER bridges the gap between analytical polarization moderation and modern learning-based network intervention.

2.1 Opinion Polarization and Moderation

Opinion polarization. Opinion polarization in online social systems is commonly studied through social influence and opinion formation models. A foundational computational framework is the Friedkin–Johnsen (FJ) model [2], where each user maintains a persistent *internal* opinion and iteratively forms an *expressed* opinion as a weighted average of her own internal belief and her neighbors’ expressed opinions. Under mild conditions, the system converges to a unique steady state. Building on this model, Matakos et al. [1] introduced a principled *polarization index* defined on the steady-state expressed opinion vector, $\pi(z) = \|z\|_2^2/n$, and provided an interpretation via absorbing random walks and

the influence operator $Q = (L + I)^{-1}$ mapping internal to expressed opinions ($z = Qs$). This formulation captures the echo-chamber phenomenon: polarization becomes high when graph communities align with homogeneous extreme internal opinions, and remains low when opinions are well-mixed across communities.

The MI/ME moderation problems. Within this framework, Matakos et al. [1] formalized two canonical moderation problems. In MODERATEINTERNAL (MI), a budgeted subset of users is selected and their internal opinions are neutralized to minimize $\pi(z)$. In MODERATEEXPRESSED (ME), a budgeted subset of users is selected and their expressed opinions are directly fixed to neutral. Both problems are NP-hard and the objective is non-monotone in the selected set, making naive greedy reasoning unreliable [1]. These formulations have become the standard benchmarks for direct opinion moderation within the FJ paradigm.

Algorithms and limitations under the FJ model. To solve MI and ME, Matakos et al. [1] proposed model-aware heuristics that exploit the linear-algebraic structure of the FJ steady state. For MI, Binary Orthogonal Matching Pursuit (BOMP) leverages the global influence operator to guide node selection and can achieve strong performance in strictly linear settings. However, this global reasoning induces scalability challenges: selection requires manipulating dense influence information, yielding complexity on the order of $O(kn^2)$, which becomes prohibitive for large networks. For ME, greedy-style strategies and lightweight heuristics such as *ExtremeExpressed* and *ExtremeNeighbors* were proposed. These approaches typically require recomputing or approximating steady-state opinions after each intervention step in order to rescore candidates, introducing substantial per-step overhead.

More importantly, these algorithms critically depend on linear steady-state analysis. Once cost-aware constraints, nonlinear opinion dynamics, or topology-altering interventions are introduced, closed-form influence operators may no longer exist or may become analytically intractable. This limits the direct applicability of model-specific heuristics beyond the original linear FJ setting.

Depolarization via exposure and topology modification. Beyond direct opinion moderation, related work has explored reshaping exposure patterns or network topology to reduce polarization. Representative approaches include adding cross-cutting edges [5, 6], optimizing edge additions under disagreement objectives [7], and studying adversarial or strategic behaviors within FJ-style dynamics [8]. Recent learning-based approaches also model depolarization as a sequential decision problem and learn policies from simulated interactions [9]. These works highlight the diversity of intervention primitives but do not provide a unified framework that scales across MI/ME-style direct moderation and FJ-consistent extensions.

2.2 Traditional Network Intervention Algorithms

The broader problem of identifying influential or critical nodes has been extensively studied in network science under tasks such as key-player identification, critical node detection, and network dismantling. The critical node problem aims to remove a limited number of nodes to maximally disrupt connectivity, with early formulations developed in operations research [10]. Subsequent work proposed scalable dismantling strategies motivated by percolation and robustness analysis [11].

Traditional intervention algorithms generally fall into several categories:

- **Greedy approaches**, which iteratively select nodes based on immediate objective improvement;
- **Spectral and relaxation methods**, leveraging eigen-structure of graph matrices;
- **Message-passing techniques**, exploiting approximate local factorization;
- **Combinatorial optimization**, including integer programming formulations.

While powerful for purely structural objectives such as connectivity or fragmentation, these methods typically do not incorporate evolving dynamical state variables such as opinions, nor do they model history-dependent intervention effects. In polarization moderation, the objective depends on the steady state of an opinion dynamics process, and the most influential nodes are not necessarily those that maximize structural centrality or connectivity disruption. This mismatch motivates learning-based planners capable of jointly reasoning about structure, dynamics, and intervention history.

2.3 Graph Reinforcement Learning on Networks

Recent advances in deep reinforcement learning (DRL) have enabled learning-based solutions to combinatorial optimization on graphs, particularly for sequential decision problems where myopic greedy choices can be suboptimal.

A representative breakthrough is FINDER [4], which formulates network dismantling as a Markov decision process and learns removal policies using deep Q-learning with graph neural encoders. FINDER demonstrated that an agent trained on small synthetic graphs can generalize to much larger real networks, achieving strong empirical scalability.

However, most graph-RL frameworks focus on *structural* objectives under *topology-altering* interventions. In contrast, opinion moderation tasks involve *dynamical state evolution* and may be *topology-preserving*: the underlying graph often remains invariant while only node attributes (internal or expressed opinions) and intervention history change. This creates unique representation challenges. When topology is fixed, distinct intervention histories may yield graph observations that appear identical if history is not explicitly encoded, resulting in state aliasing and unstable value estimation. Furthermore, when opinions are continuous-valued or governed by nonlinear but topology-preserving dynamics, structural encoders alone may be insufficient to capture polarization-relevant signals.

2.4 Research Gap and Our Contribution

Despite advances in polarization moderation and graph reinforcement learning, a methodological gap remains. Model-specific analytical approaches provide strong guarantees in strictly linear settings but lack flexibility and scalability under cost-aware, nonlinear, or topology-changing regimes. Conversely, graph-RL methods offer scalable inductive learning paradigms but have largely focused on structural objectives rather than dynamical polarization minimization.

PACIFIER bridges this gap by formulating MODERATEINTERNAL and MODERATEEXPRESSED—and their FJ-consistent extensions—as sequential decision problems over networked opinion dynamics. Our framework is objective-agnostic and accommodates multiple intervention paradigms, including cost-aware moderation, biased-assimilation dynamics, and node removal, while preserving the underlying influence topology when appropriate. To address topology-preserving aliasing, we introduce a temporal-aware node marking mechanism, and to enhance value estimation, we incorporate polarization-aware global features.

Empirically, this unified graph-RL formulation not only remains competitive with near-optimal analytical solvers in strictly linear MI settings, but also substantially outperforms classical baselines in cost-aware, nonlinear, and topology-altering regimes, where steady-state-based heuristics lose structural advantages. This establishes a scalable and extensible learning-based paradigm for opinion polarization moderation.

3 Problem Formulation: MI/ME Moderation under the Friedkin–Johnsen Paradigm: One-Shot Planning and ANP Evaluation

This section formally defines the opinion polarization moderation problems studied in this work. We begin by reviewing the Friedkin–Johnsen (FJ) opinion dynamics model and the associated polarization index. We then define the MODERATEINTERNAL and MODERATEEXPRESSED problems under this model. Finally, we introduce our *one-shot planning constraint*—which requires committing to a complete intervention sequence using only the initial instance information—and the *accumulated normalized polarization (ANP)* evaluation metric that measures the area-under-curve of polarization along the intervention trajectory, together characterizing the setting targeted by our PACIFIER framework.

3.1 Friedkin-Johnsen Opinion Dynamics Model

We consider a social network represented as an undirected, weighted graph $G = (V, E)$, where $|V| = n$ denotes the set of individuals and E represents the social ties between them. Each edge $(i, j) \in E$ is associated with a weight $w_{ij} \geq 0$, signifying the strength of influence between individuals i and j . Each individual $i \in V$ also has a *self-weight* $w_{ii} > 0$, which quantifies their level of attachment to their own internal belief.

The opinion formation process is governed by the Friedkin–Johnsen (FJ) model [2]. In this model, each individual i maintains two types of opinions:

- **Internal opinion** (s_i): a persistent belief, represented as a scalar value. In our setting, $s_i \in [-1, 1]$, where -1 and 1 represent two opposing extreme stances, and 0 represents a neutral stance.
- **Expressed opinion** (z_i): a publicly stated opinion that evolves over time based on social influence.

The update rule for the expressed opinion of individual i is a weighted average of their own internal opinion and the current expressed opinions of their neighbors:

$$z_i = \frac{w_{ii}s_i + \sum_{j \in N(i)} w_{ij}z_j}{w_{ii} + \sum_{j \in N(i)} w_{ij}}, \quad (1)$$

where $N(i)$ denotes the set of neighbors of node i in G . It is well-established that this iterative process converges to a unique *steady-state* expressed opinion vector \mathbf{z} for any initial condition.

The steady-state vector \mathbf{z} can be computed directly in closed form using the network structure and the internal opinion vector \mathbf{s} . Let L be the Laplacian matrix of graph G . The fundamental matrix Q is defined as:

$$Q = (L + I)^{-1}. \quad (2)$$

The steady-state expressed opinions are then given by:

$$\mathbf{z} = Q\mathbf{s}. \quad (3)$$

3.2 Polarization Index

Following [1], we quantify the level of polarization in the network using the *polarization index* based on the steady-state expressed opinion vector.

Definition 3.1 (Polarization Index). Given a network $G = (V, E)$, a vector of internal opinions \mathbf{s} , and the resulting steady-state vector of expressed opinions \mathbf{z} , the polarization index $\pi(\mathbf{z})$ is defined as:

$$\pi(\mathbf{z}) = \frac{\|\mathbf{z}\|^2}{n}. \quad (4)$$

3.3 Canonical Moderation Problems

We now formalize the two key intervention problems for reducing polarization. Throughout, we assume a budget k , and the goal is to select k individuals to *moderate*, i.e., to set the targeted opinion attribute to a neutral state (0), such that the resulting polarization index is minimized.

Base vs. continuous opinion settings. We distinguish two closely related opinion settings. (i) *Base setting* (Matakos *et al.*). The internal opinions are binary and polarized, i.e., $s_i \in \{-1, +1\}$, where -1 and $+1$ represent two opposing camps and 0 denotes neutrality after moderation. (ii) *Continuous setting* (our extension). The internal opinions are continuous, $s_i \in [-1, 1]$, which allows heterogeneous opinion intensities. The two opposing camps correspond to negative vs. positive opinions, i.e., $s_i \in (-1, 0)$ and $s_i \in (0, 1)$, with $s_i = 0$ representing the neutral stance. In both settings, the moderation action sets the targeted attribute to 0 for selected individuals; the continuous setting generalizes the base setting by allowing magnitudes between the extremes.

3.3.1 The MODERATEINTERNAL Problem

Problem 3.1 (MODERATEINTERNAL). Given a graph $G = (V, E)$, an internal opinion vector $\mathbf{s} \in [-1, 1]^n$ (binary in the base setting, continuous in our extension), and an integer budget $k > 0$, find a set $T_s \subset V$ with $|T_s| = k$ such that the polarization index is minimized after setting $s_i = 0$ for all $i \in T_s$. Let \mathbf{s}' denote the modified internal opinion vector, and let \mathbf{z}' be the resulting steady-state expressed opinion vector under the FJ model (i.e., $\mathbf{z}' = Q\mathbf{s}'$ in the linear case). The objective is:

$$\min_{T_s \subset V, |T_s|=k} \pi(\mathbf{z}') = \frac{1}{n} \|Q\mathbf{s}'\|^2.$$

3.3.2 The MODERATEEXPRESSED Problem

Problem 3.2 (MODERATEEXPRESSED). Given a graph $G = (V, E)$, an internal opinion vector \mathbf{s} (binary in the base setting, continuous in our extension), the corresponding steady-state expressed opinion vector \mathbf{z} , and an integer budget $k > 0$, find a set $T_z \subset V$ with $|T_z| = k$ such that the polarization index is minimized after fixing $z_i = 0$ for all $i \in T_z$. The dynamics are recalculated under this constraint, leading to a new steady-state vector \mathbf{z}' . The objective is:

$$\min_{T_z \subset V, |T_z|=k} \pi(\mathbf{z}') = \frac{1}{n} \|\mathbf{z}'\|^2.$$

3.4 Our Setting: One-Shot Planning with ANP Evaluation

The canonical MI/ME formulations above specify *what* is being intervened on, but do not specify *what information* a planning algorithm may use while constructing the intervention trajectory. Here we study a setting with two coupled components: a *one-shot planning constraint* and an *accumulated normalized polarization (ANP) evaluation metric*.

(i) One-shot planning constraint (plan once from the initial instance). Let $\mathbf{z}^{(0)}$ denote the converged expressed-opinion vector (i.e., the FJ *settled opinions*) under the original instance, so $\mathbf{z}^{(0)} = \mathbf{z}$ in (3). The planner observes only the *initial* instance information

$$\mathcal{I}_0 = (G, \mathbf{s}, \mathbf{z}^{(0)}, k) \quad (\text{and costs if applicable}),$$

and must output a complete ordered intervention sequence

$$(v_1, \dots, v_k)$$

in a single planning pass.

Crucially, executing an action changes the opinion system. For MI, intervening on v_t modifies the internal opinion (stubbornness anchor) of that node, e.g., $s(v_t) \leftarrow 0$; for ME, intervening on v_t fixes the expressed opinion of that node, e.g., $z(v_t) \leftarrow 0$, which acts as an exogenous constraint in the subsequent opinion-formation process. If one were to execute the first t actions and then re-run the opinion dynamics to convergence, one would obtain a new limiting vector of settled opinions, denoted by $\mathbf{z}^{(t)}$.

Under the one-shot constraint, such intermediate settled-opinion states are *not available* to the planner during selection: the algorithm is **not allowed** to recompute, query, or otherwise use any $\mathbf{z}^{(t)}$ induced by partial prefixes $\{v_1, \dots, v_t\}$. Equivalently, the planned sequence must be a function of \mathcal{I}_0 alone,

$$(v_1, \dots, v_k) = \Pi(\mathcal{I}_0),$$

Why one-shot planning? A key property of MI/ME-style moderation is that it is *topology-preserving*: the social graph is treated as fixed, and interventions act on opinion-related attributes (internal or expressed) rather than rewiring links. At the same time, polarization is tightly coupled with echo-chamber structure—when opposing camps are well-separated by the topology, the steady-state opinions tend to become more extreme and more segregated. This coupling makes multi-round “intervene–re-equilibrate–replan” pipelines problematic in two ways. First, they are computationally expensive because each additional round requires re-solving (or simulating) the opinion dynamics to a settled state, which becomes a major bottleneck on large graphs and can be infeasible under nonlinear or non-analytic dynamics. Second, repeated replanning is methodologically misaligned with deployment: it implicitly assumes the influence topology remains stable long enough for opinions to settle after every partial intervention, whereas real platforms may exhibit structural drift or co-evolution over the same horizon, undermining the validity of repeatedly conditioning on intermediate equilibria. These considerations motivate a *plan-once* regime: the planner commits to a complete ordered intervention sequence using only the initial instance information, while intermediate settled-opinion states are computed *only* for evaluation.

What this rules out. This explicitly excludes “select-and-recompute” heuristics for MI/ME that repeatedly: (a) apply one intervention, (b) re-equilibrate the dynamics to obtain the new settled opinions, and then (c) use the updated settled-opinion state to score and select the next node.

(ii) Accumulated normalized polarization (ANP) evaluation metric (area-under-curve). Although planning is restricted as above, we evaluate a produced sequence (v_1, \dots, v_k) using an accumulated score that rewards *earlier* and *more consistent* polarization reduction along the trajectory. Let $\mathbf{z}^{(t)}$ denote the converged expressed-opinion vector (the settled opinions) *for evaluation purposes* after applying the first t interventions in the sequence, for $t = 0, 1, \dots, k$.

We view the budget horizon as a normalized progress axis:

$$x_t = \frac{t}{k} \in [0, 1],$$

so the full sequence (v_1, \dots, v_k) traces a polarization trajectory from $x_0 = 0$ (no intervention) to $x_k = 1$ (all k interventions executed). We define the normalized polarization at step t as

$$\hat{\pi}(\mathbf{z}^{(t)}) = \frac{\pi(\mathbf{z}^{(t)})}{n}, \quad (5)$$

where $\pi(\mathbf{z}) = \|\mathbf{z}\|_2^2/n$ is the polarization index in (4). Then the accumulated normalized polarization (ANP) score is defined as the discrete area-under-curve proxy:

$$\mathcal{R}_{\text{ANP}}(v_1, \dots, v_k) = \frac{1}{k} \sum_{t=0}^k \hat{\pi}(\mathbf{z}^{(t)}). \quad (6)$$

Intuitively, \mathcal{R}_{ANP} approximates the area under the polarization curve $\hat{\pi}(\mathbf{z}^{(t)})$ over the normalized horizon $x \in [0, 1]$. Lower values indicate that polarization is reduced *earlier* (small values for small t) and *persistently* (small values throughout the trajectory), rather than only near the end.

Implication. Our setting is sequential (since the output is an ordered trajectory and every prefix contributes to evaluation), but the planner is one-shot: it commits to the entire sequence based only on initial instance information, and the sequence is then directly evaluated under the ANP (area-under-curve) criterion emphasizing *when* polarization reduction occurs.

3.5 Computational Complexity

Both MI and ME are computationally challenging, as established in [1].

Theorem 3.1 ([1]). *The MODERATEINTERNAL problem is NP-hard.*

Theorem 3.2 ([1]). *The MODERATEEXPRESSED problem is NP-hard.*

3.6 Extensibility Beyond the Linear FJ Model

The formulations above are presented under the linear Friedkin–Johnsen (FJ) model for clarity. However, a central motivation of this work is to develop a moderation framework that is *not tied to a specific analytical form* of the opinion dynamics. In this subsection, we clarify the class of extensions considered in this paper and illustrate how PACIFIER naturally generalizes beyond the linear FJ setting.

FJ-consistent extensions. We focus on extensions that preserve the core social influence structure of the FJ model—namely, influence propagation along the edges of the social network and the distinction between internal and expressed opinions—while relaxing either the *network topology* or the *opinion update rule*. Importantly, these extensions may break linearity and analytical tractability, but remain compatible with PACIFIER because the framework does not rely on closed-form solutions.

Topology-altering interventions: node removal. As a first class of extensions, we consider *Topology-altering interventions* that explicitly modify the network topology. In particular, removing a node eliminates both its incoming and outgoing influence, resulting in a dynamically changing graph structure. This setting is analogous to classical network dismantling problems and serves as a bridge between opinion moderation and structural network intervention. Unlike MI and ME, where the topology remains fixed, node removal alters the Laplacian matrix itself and invalidates precomputed influence matrices such as $Q = (L + I)^{-1}$. PACIFIER naturally accommodates this setting by operating directly on the evolving graph state rather than relying on static influence operators.

Dynamics-altering interventions: biased assimilation. As a second class of extensions, we consider nonlinear variants that retain the original topology but modify the opinion update rule. A representative example is the *biased assimilation* model proposed by [12], which captures the tendency of individuals to overweight information that aligns with their current beliefs. The update rule for an individual i is given by

$$x_i(t+1) = \frac{w_{ii}x_i(t) + (x_i(t))^b s_i(t)}{w_{ii} + (x_i(t))^b s_i(t) + (1 - x_i(t))^b (d_i - s_i(t))}, \quad (7)$$

where $b \geq 0$ controls the strength of confirmation bias. For $b \geq 1$, this model generates strong polarization effects but generally lacks a closed-form steady-state solution.

Implications for PACIFIER. Both extensions highlight a key limitation of model-specific moderation algorithms: once linearity is lost or interventions alter the topology, approaches that rely on repeated matrix inversions (such as BOMP) or analytical steady-state expressions (such as ExtremeExpressed) become infeasible. In contrast, PACIFIER treats opinion dynamics as a black-box environment and evaluates interventions solely through their observed impact on polarization. As a result, the same learning-based framework can be applied without modification to linear and nonlinear dynamics, as well as to topology-preserving and topology-altering interventions. These extensions therefore serve not as separate problem formulations, but as evidence of the generality and flexibility of the proposed approach.

4 PACIFIER Framework

PACIFIER is a graph-based learning framework for sequential polarization moderation on networks. It is designed to learn intervention policies from simulated interactions and deploy them efficiently on large real-world graphs. The framework follows a two-phase workflow: (i) offline training on synthetic graph–opinion instances, and (ii) feed-forward deployment on target networks without iterative recomputation during planning.

PACIFIER supports two closely related variants within the same architecture: **PACIFIER-RL**, which learns a long-horizon intervention policy via bootstrapped reinforcement learning, and **PACIFIER-Greedy**, a myopic variant that learns to approximate immediate polarization reduction without bootstrapping. Both variants share the same encoder–decoder representation and differ only in their training objectives.

Design principles. Polarization moderation under MI/ME-type interventions differs fundamentally from topology-altering structural control. In many practical settings, the graph topology remains fixed, while polarization evolves through opinion dynamics and intervention history. This shift motivates three core design principles underlying PACIFIER:

- **Structured episode generation (two-echo-chamber initialization).** Each training episode is initialized from a synthetic graph with two communities (echo chambers) and an aligned opinion assignment. Nodes are partitioned into V^+ and V^- , dense within-group connections are generated with controllable sparse cross-group exposure, and internal opinions are initialized according to community membership (e.g., $s_i^{(0)} = +1$ for $i \in V^+$ and $s_i^{(0)} = -1$ for $i \in V^-$). Varying the inter-group edge ratio yields controllable polarization regimes and exposes the policy to diverse yet structured states.
- **Trajectory-aware reward design (optionally cost-weighted).** Rather than optimizing only a terminal objective, PACIFIER assigns stepwise rewards that encourage reducing polarization early along the intervention sequence. Node-specific intervention costs can be incorporated naturally, allowing the framework to balance polarization reduction against heterogeneous moderation effort.
- **History-aware and polarization-aware representations.** Because the topology may remain unchanged across decision steps, intervention history cannot be inferred from structure alone. PACIFIER therefore explicitly encodes intervention history at the node level to prevent history-induced state aliasing. In addition, it augments learned graph embeddings with polarization-related auxiliary features that capture opinion–structure interaction patterns, providing value-relevant global signals for stable policy learning.

These components jointly enable PACIFIER to learn scalable intervention strategies that generalize from small synthetic graphs to large real-world networks while maintaining lightweight inference at deployment time.

4.1 Framework

We follow the inductive graph-RL paradigm of FINDER and adopt the same two-phase workflow: (i) *offline training* on synthetic instances, and (ii) *online (deployment-time) application* on a target real network, where inference is a lightweight feed-forward scoring of all candidate nodes.

We instantiate two closely related variants within the same architecture: **PACIFIER-RL**, which adopts multi-step Q-learning with bootstrapping, and **PACIFIER-Greedy**, a simplified myopic variant that learns only from immediate rewards without bootstrapping.

MDP formulation. We model sequential polarization moderation as a Markov Decision Process (MDP) over a graph with evolving node attributes. At each decision step, the agent selects one node to intervene on, observes the resulting state transition, and receives a reward that reflects the evaluated polarization after the intervention. An episode corresponds to a full intervention trajectory of length k (or until no feasible actions remain).

State. At step t , the state is

$$s_t = (G, X_t, \mathbf{u}_t, \mathbf{m}_t),$$

where $G = (V, E)$ is the (fixed) network, $X_t \in \mathbb{R}^{n \times d_x}$ is the node-feature matrix, $\mathbf{u}_t \in \mathbb{R}^{d_u}$ is a graph-level auxiliary feature vector, and $\mathbf{m}_t \in \{0, 1\}^n$ is an action-feasibility mask. Let $S_t \subseteq V$ denote the set of already intervened nodes. Then $\mathbf{m}_t(v) = 0$ for $v \in S_t$ and $\mathbf{m}_t(v) = 1$ otherwise.

Under MI/ME-style moderation, the topology of G remains fixed. State evolution is therefore driven by opinion updates and intervention history, which is explicitly encoded in X_t (Sec. 4.3).

Action. An action selects one feasible node:

$$a_t \in \mathcal{A}_t = \{v \in V \mid \mathbf{m}_t(v) = 1\}.$$

For MI-style intervention, executing a_t sets $s_t(a_t) \leftarrow 0$. Other intervention mechanisms (e.g., fixing expressed opinions or node removal) modify only the environment transition while preserving the decision interface.

Transition. After applying the intervention, we update $S_{t+1} = S_t \cup \{a_t\}$ and the feasibility mask accordingly. For topology-preserving settings, G remains unchanged. For topology-altering extensions (e.g., node removal), G is updated.

Reward (trajectory-aware signal). Let $\pi(\mathbf{z}^{(t)})$ denote the polarization index computed from the converged expressed opinions after t interventions. In cost-weighted settings, each node has cost $c(v)$ and $C = \sum_{v \in V} c(v)$. The step reward is defined as

$$r_t = -\frac{\pi(\mathbf{z}^{(t)})}{C} \cdot c(a_t).$$

For unweighted settings, $c(v) \equiv 1$.

Policy parameterization via encode–decode. Both PACIFIER-RL and PACIFIER-Greedy share the same architecture. The encoder produces node embeddings $\{\mathbf{h}_v\}$ and a graph-level embedding \mathbf{g}_t from (G, X_t) , together with auxiliary features \mathbf{u}_t (Sec. 4.3). The decoder maps $(\mathbf{h}_v, \mathbf{g}_t, \mathbf{u}_t)$ to an action-value estimate $Q_\theta(s_t, v)$ for each node (Sec. 4.4). Feasibility is enforced via \mathbf{m}_t .

Offline training. PACIFIER-RL. During offline training, PACIFIER-RL interacts with sampled synthetic instances from \mathcal{D} to generate trajectories $\{(s_t, a_t, r_t, s_{t+1})\}$ over a fixed horizon (budget) k (or until no feasible action remains). At each step, the agent observes the state representation $(G, X_t, \mathbf{u}_t, \mathbf{m}_t)$ and selects one feasible node via an ϵ -greedy strategy: with probability $1 - \epsilon$ it chooses the feasible node with the largest predicted $Q_\theta(s_t, v)$, and otherwise samples a feasible node uniformly at random. The exploration rate ϵ is annealed from a high initial value to a small final value over training episodes.

We adopt n -step Q-learning with experience replay. We store transitions $(s_t, a_t, R_{t:t+n}, s_{t+n})$ in a replay buffer, where the truncated return is

$$R_{t:t+n} = \sum_{i=0}^{n-1} \gamma^i r_{t+i}.$$

The TD target is computed using a periodically updated target network:

$$y_t = R_{t:t+n} + \gamma^n \max_v Q_{\theta^-}(s_{t+n}, v),$$

where θ^- denotes the target-network parameters. The encoder–decoder parameters θ are optimized by minimizing the mean-squared TD error:

$$\mathcal{L}_{\text{RL}}(\theta) = \mathbb{E} \left[(Q_\theta(s_t, a_t) - y_t)^2 \right].$$

Mini-batches are sampled uniformly from the replay buffer and parameters are updated using Adam. We employ standard stabilizers for deep Q-learning, including (i) experience replay, (ii) a target network, and (iii) n -step returns.

For training signal, the environment computes the converged expressed-opinion state after each intervention (under the specified opinion dynamics) and evaluates the polarization index $\pi(\mathbf{z}^{(t)})$ to produce reward r_t . Crucially, this converged computation is used *only* inside the environment to generate rewards and learning targets; the policy input remains $(G, X_t, \mathbf{u}_t, \mathbf{m}_t)$ and thus does not require repeated steady-state recomputation during planning, aligning with our non-iterative planning constraint.

PACIFIER-Greedy. The greedy variant removes bootstrapping and multi-step returns and learns only from immediate rewards. We store 1-step tuples (s_t, a_t, r_t) and set the learning target as

$$y_t = r_t.$$

Parameters are optimized by minimizing

$$\mathcal{L}_{\text{Greedy}}(\theta) = \mathbb{E} \left[(Q_\theta(s_t, a_t) - r_t)^2 \right].$$

During training, PACIFIER-Greedy performs *pure exploration* by sampling actions uniformly at random from feasible nodes, i.e., $a_t \sim \text{Unif}(\mathcal{A}_t)$, without any ϵ -greedy scheduling or annealing. Thus, PACIFIER-Greedy learns a myopic value estimator that approximates the immediate polarization-reduction effect of each intervention.

Online application (deployment). After offline training, both variants are deployed on a target real-world graph in a purely *feed-forward* manner. At each decision step t , we construct the current state representation $(G, X_t, \mathbf{u}_t, \mathbf{m}_t)$ and evaluate $Q_\theta(s_t, v)$ for all nodes in parallel. Feasibility is enforced by the mask \mathbf{m}_t : nodes with $\mathbf{m}_t(v) = 0$ (already intervened) are assigned a large negative value and are never selected. The deployed policy is greedy with respect to Q_θ :

$$a_t = \arg \max_{v \in V} Q_\theta(s_t, v) \quad \text{s.t. } \mathbf{m}_t(v) = 1.$$

This yields an ordered intervention sequence (v_1, \dots, v_k) and requires no additional optimization at test time. Importantly, online application does *not* require repeated steady-state recomputation during planning: while the environment may compute converged expressed opinions for evaluation, the deployed policy relies only on the learned representations and the intervention history encoded in $(X_t, \mathbf{u}_t, \mathbf{m}_t)$.

4.2 Two-Echo-Chamber Training Instance Distribution

PACIFIER follows an inductive learning paradigm and is trained offline on a distribution of synthetic graph–opinion instances. The purpose of this distribution is not to exactly replicate any single real-world network, but to expose the agent to a diverse yet structured set of polarized states that capture the dominant regimes observed in practice.

Two-echo-chamber episode initialization. Each training episode begins by sampling an initial instance

$$(G, \mathbf{s}^{(0)}, \mathbf{c}) \sim \mathcal{D},$$

where $G = (V, E)$ is a graph, $\mathbf{s}^{(0)} \in [-1, 1]^n$ is the initial internal-opinion vector, and $\mathbf{c} \in \mathbb{R}_{\geq 0}^n$ is an optional vector of intervention costs (with $\mathbf{c} \equiv \mathbf{1}$ in the unweighted setting). The distribution \mathcal{D} is designed to generate graph–opinion configurations with diverse yet controlled polarization characteristics.

Graph size and community partition. To facilitate inductive generalization, training graphs are generated at relatively small scales. For topology-preserving settings (e.g., MI and ME), the total number of nodes is sampled uniformly from the range $n \in [18, 50]$. For topology-altering settings such as node removal, we use slightly larger graphs with $n \in [30, 50]$ to ensure sufficient structural variability after removals. In all cases, the node set V is partitioned into two disjoint subsets V^+ and V^- of equal size (or differing by at most one node when n is odd), representing two opposing echo chambers.

Graph structure generation. To generate polarized yet realistic network structures, we construct G using a two-group generative process based on the Barabási–Albert (BA) preferential-attachment model. On each subset V^+ and V^- , we independently generate a scale-free subgraph using the BA model, yielding heterogeneous degree distributions within each group.

To control the strength of cross-group exposure, we then add a set of inter-group edges between V^+ and V^- . The number of such edges is sampled as a fraction of the total number of intra-group edges, and each inter-group edge connects a node chosen uniformly at random from V^+ to one chosen uniformly at random from V^- . By varying the inter-group edge ratio, this procedure produces graphs ranging from highly segregated (strong polarization) to weakly mixed (low polarization), while preserving scale-free degree characteristics.

Internal opinion initialization. Given the generated graph G , internal opinions are initialized according to the group assignment:

$$s_i^{(0)} = \begin{cases} +1, & i \in V^+, \\ -1, & i \in V^-. \end{cases}$$

This alignment between network communities and opinion camps serves as a canonical polarized starting point. For continuous-opinion settings, this initialization can be extended by sampling opinion magnitudes from bounded continuous distributions with the same sign structure, or by adding controlled noise.

Intervention cost initialization. For cost-weighted intervention settings, each node $i \in V$ is assigned a nonnegative intervention cost c_i , independently sampled from a fixed distribution. The cost represents the relative difficulty or expense of moderating node i . In unweighted settings, all nodes are assigned unit cost.

Empirical motivation from real-world polarized graphs. To justify the above synthetic training distribution, we analyze the real-world Twitter follow and retweet graphs used in our experiments. For each dataset, nodes are partitioned

into two camps according to the sign of their internal-opinion labels, and we compute a set of partition-aware structural statistics.

Across datasets, we observe that these statistics consistently fall within the range spanned by the synthetic BA-based two-group graphs generated by \mathcal{D} . In particular, real graphs exhibit (i) strong within-camp connectivity, (ii) sparse but non-negligible cross-camp exposure, and (iii) degree heterogeneity compatible with preferential-attachment structure. These observations indicate that the proposed training distribution captures the dominant polarization regimes present in real data, thereby narrowing the train–test distribution gap and improving generalization.

4.3 Encoding

The encoding module maps the current moderation state into vector representations that can be reused to score all candidate nodes efficiently. Compared with topology-altering intervention tasks (e.g., node removal), MI/ME-type moderation is typically *topology-preserving*: the underlying graph topology remains unchanged across decision steps, while only node attributes (opinions) and the intervention history evolve over time.

Definition 4.1 (Topology-preserving intervention). An intervention process is *topology-preserving* if, throughout the decision horizon, the graph topology remains exactly unchanged: no nodes or edges are removed, added, rewired, or reweighted, and hence no node or edge becomes structurally inactive. Formally, the graph structure $G = (V, E)$ is invariant (i.e., V and E do not change with t), and the intervention only modifies node/edge *attributes* or imposes *constraints* (e.g., internal opinions, expressed opinions, or fixed-value boundary conditions). In such settings, the adjacency structure alone cannot reveal which nodes have been intervened on, creating a representation ambiguity under permutation-invariant message-passing GNN encoders, where different intervention histories can produce nearly identical aggregated embeddings, leading to state aliasing and degraded value estimation in reinforcement learning.

This topology-preserving setting gives rise to two fundamental representation challenges: (i) *history-induced state aliasing* under a fixed topology, and (ii) the lack of *polarization-related global signals* in standard message-passing representations, which can hinder accurate value estimation and stable policy learning when polarization is driven by nontrivial interactions between opinion states and network structure. PACIFIER addresses these challenges via two encoding innovations: a temporal-aware node marking mechanism to explicitly encode intervention history, and polarization-related auxiliary features that summarize opinion–structure interaction patterns to provide value-relevant global cues.

State. At decision step t , the environment state is represented as

$$s_t = (G, X_t, \mathbf{u}_t, \mathbf{m}_t),$$

where $G = (V, E)$ is the (fixed) network, $X_t \in \mathbb{R}^{n \times d_0}$ is the node-feature matrix, $\mathbf{u}_t \in \mathbb{R}^{d_u}$ is a graph-level auxiliary feature vector, and $\mathbf{m}_t \in \{0, 1\}^n$ is a feasibility mask indicating which nodes can still be selected for intervention.

Encoding pipeline overview (graph + node features + super-node aggregation). Figuratively, PACIFIER’s encoder takes as input (i) the fixed adjacency structure of G and (ii) per-node attributes that evolve with interventions, and produces node embeddings and a graph-level embedding that are reused to score all actions in parallel. The pipeline is summarized as follows.

(1) Inputs. We represent the graph structure through a (sparse) neighbor-sum operator induced by the adjacency matrix, and represent the evolving moderation status through node features X_t (defined below). In addition, we maintain a *super-node* (a virtual graph token) that is connected to all nodes by directed edges from nodes to the super-node; its role is to aggregate a graph-level summary at each message-passing iteration.

(2) Feature-to-embedding projection (node initialization). Each node feature vector $\mathbf{x}_t(v)$ is first mapped into a latent embedding via a shared linear projection and nonlinearity:

$$\mathbf{h}_v^{(0)} = \sigma(W_0 \mathbf{x}_t(v)), \quad \mathbf{h}_v^{(0)} \leftarrow \text{norm}(\mathbf{h}_v^{(0)}), \quad (8)$$

where $\text{norm}(\cdot)$ denotes ℓ_2 normalization. This corresponds to the input projection layer in our implementation (the w_{n2l} mapping).

(3) GraphSAGE message passing (node updates). For $k = 1, \dots, K$, nodes aggregate their neighbors’ embeddings and update their own embeddings in a GraphSAGE-style manner:

$$\mathbf{a}_v^{(k)} = \sum_{u \in \mathcal{N}(v)} \mathbf{h}_u^{(k-1)}, \quad (9)$$

$$\mathbf{h}_v^{(k)} = \sigma \left(W_{\text{sage}} \begin{bmatrix} W_{\text{nbr}} \mathbf{a}_v^{(k)} \\ W_{\text{self}} \mathbf{h}_v^{(k-1)} \end{bmatrix} \right), \quad \mathbf{h}_v^{(k)} \leftarrow \text{norm}(\mathbf{h}_v^{(k)}). \quad (10)$$

This design matches the implementation pattern: a sparse neighbor-sum (`n2nsum_param`) followed by linear transforms (`p_node_conv`, `p_node_conv2`) and a concatenation-based update (`p_node_conv3`).

(4) Super-node update (graph-level aggregation at each iteration). In parallel with node updates, the super-node aggregates current node embeddings by a global sum pooling operator:

$$\mathbf{g}^{(k)} = \sum_{v \in V} \mathbf{h}_v^{(k)}, \quad (11)$$

which provides an iteration-synchronized global summary of the evolving opinion/intervention state. In our implementation, this is realized by an explicit aggregation operator (a sparse `subgsum_param` that pools node embeddings into a batch-level vector), conceptually equivalent to a virtual node connected to all nodes and updated by one-way aggregation.

(5) Encoder outputs. After K iterations, the encoder outputs: (i) node embeddings $\{\mathbf{h}_v\}_{v \in V}$ with $\mathbf{h}_v = \mathbf{h}_v^{(K)}$, and (ii) a graph-level embedding \mathbf{g}_t (we use $\mathbf{g}_t = \mathbf{g}^{(K)}$), together with (iii) deterministic auxiliary features \mathbf{u}_t and (iv) a feasibility mask \mathbf{m}_t . These outputs are shared across all candidate actions and are consumed by the decoding module to compute $Q(s_t, v)$ for every node v .

Node features (temporal-aware marking; Innovation 1). Let $S_t \subseteq V$ denote the set of nodes that have already been intervened by step t . In topology-preserving moderation, the adjacency structure alone does not encode intervention history; consequently, different intervention sequences may produce graph states that are indistinguishable if history is not explicitly represented. This *state aliasing* can severely degrade value estimation and credit assignment in sequential decision making.

To resolve this issue, PACIFIER explicitly encodes intervention history into node features via a temporal-aware marking mechanism. Each node v is assigned a feature vector

$$\mathbf{x}_t(v) = [s_t(v), s_0(v), \text{mark}_t(v), c(v)], \quad (12)$$

where $s_t(v)$ is the current opinion attribute after previous interventions, $s_0(v)$ is the initial opinion attribute at the beginning of the episode, $\text{mark}_t(v) = \mathbb{I}[v \in S_t]$ indicates whether node v has already been intervened, and $c(v) \geq 0$ denotes an optional node-specific intervention cost (set to a constant in unweighted settings). The feasibility mask is consistent with the marking feature:

$$\mathbf{m}_t(v) = 1 - \text{mark}_t(v),$$

so nodes that have already been selected are excluded from future actions.

Polarization-related auxiliary features (Innovation 2). While learned embeddings capture rich local and global structure, polarization moderation objectives depend explicitly on how the opinion configuration interacts with the network. Purely message-passing representations can be insufficient to expose the global signals that correlate with polarization regimes (e.g., cross-camp exposure among remaining active nodes, or the level of within-camp cohesion), especially under one-shot planning where the policy input should not rely on repeated steady-state recomputation.

We therefore augment learned embeddings with a deterministic auxiliary feature vector \mathbf{u}_t that summarizes intervention progress and opinion–structure interaction patterns. Concretely, let $n = |V|$ and $m = |E|$. We include the covered-node ratio

$$u_t^{(1)} = \frac{|S_t|}{n}. \quad (13)$$

Let $E_{\text{cov}}(t) = \{(i, j) \in E \mid i \in S_t \text{ or } j \in S_t\}$ denote edges incident to covered nodes. The covered-edge ratio is

$$u_t^{(2)} = \frac{|E_{\text{cov}}(t)|}{m}. \quad (14)$$

To characterize cross-camp interactions among active edges, define

$$E_{\pm}(t) = \{(i, j) \in E \setminus E_{\text{cov}}(t) \mid \text{sign}(s_t(i)) \neq \text{sign}(s_t(j))\},$$

and include

$$u_t^{(3)} = \frac{|E_{\pm}(t)|}{m}. \quad (15)$$

We further include a two-hop structural statistic on the active subgraph $G[V \setminus S_t]$. Let $d_t(v)$ denote the degree of node v in this subgraph. Define

$$T(t) = \sum_{v \notin S_t} \binom{d_t(v)}{2}, \quad u_t^{(4)} = \frac{T(t)}{n^2}. \quad (16)$$

To further capture sign-based community cohesion, we compute two-hop statistics separately within the positive and negative opinion groups. Define

$$V_t^+ = \{v \notin S_t \mid s_t(v) > 0\}, \quad V_t^- = \{v \notin S_t \mid s_t(v) \leq 0\}.$$

Let $T^+(t)$ and $T^-(t)$ denote the corresponding two-hop counts within the induced subgraphs on V_t^+ and V_t^- . We include

$$u_t^{(5)} = \frac{T^+(t)}{n^2}, \quad u_t^{(6)} = \frac{T^-(t)}{n^2}. \quad (17)$$

The complete auxiliary feature vector is

$$\mathbf{u}_t = [u_t^{(1)}, u_t^{(2)}, u_t^{(3)}, u_t^{(4)}, u_t^{(5)}, u_t^{(6)}]. \quad (18)$$

Output of encoding. The encoding stage produces (i) node embeddings $\{\mathbf{h}_v\}_{v \in V}$, (ii) a graph-level embedding \mathbf{g}_t (via super-node/global aggregation), (iii) polarization-related auxiliary features \mathbf{u}_t , and (iv) a feasibility mask \mathbf{m}_t . These representations are then passed to the decoding module to score all candidate intervention actions.

4.4 Decoding

The decoding module evaluates each feasible node as a candidate intervention based on the representations produced by the encoding stage. PACIFIER adopts a value-based decoding strategy and learns an action-value function $Q(s_t, v)$ that estimates the long-term return of selecting node v at state s_t .

State-action interaction. Given the embedding \mathbf{h}_v of a candidate node v and the graph-level embedding \mathbf{g}_t , PACIFIER models their interaction through a bilinear transformation:

$$\mathbf{z}_{t,v} = (\mathbf{h}_v \mathbf{g}_t^\top) \mathbf{w}, \quad (19)$$

where \mathbf{w} is a learnable projection vector. This interaction captures multiplicative effects between the local representation of the selected node and the global state of the network, allowing the decoder to assess how intervening on v may influence future polarization dynamics at the graph level.

Q-value prediction. The interaction vector $\mathbf{z}_{t,v}$ is concatenated with the auxiliary feature vector \mathbf{u}_t and mapped to a scalar action value via a shared nonlinear function:

$$Q(s_t, v) = f_\theta \left(\begin{bmatrix} \mathbf{z}_{t,v} \\ \mathbf{u}_t \end{bmatrix} \right), \quad (20)$$

where $f_\theta(\cdot)$ denotes a multilayer perceptron with ReLU activations. The same function is applied to all candidate nodes, ensuring parameter sharing and inductive generalization across different graphs and intervention stages.

Action masking. To enforce feasibility constraints, nodes that have already been intervened are excluded from selection by applying a large negative bias:

$$Q(s_t, v) \leftarrow Q(s_t, v) + (1 - m_t(v)) \cdot (-M), \quad (21)$$

where M is a sufficiently large constant. This guarantees that infeasible actions are never chosen during decoding.

Parallel evaluation. Because the graph-level embedding \mathbf{g}_t and the auxiliary vector \mathbf{u}_t are shared across all candidate nodes, the action-value function $Q(s_t, v)$ can be evaluated for all nodes in parallel. This design enables efficient inference on large graphs and allows PACIFIER to scale to real-world networks without enumerating actions sequentially.

4.5 Flexibility

PACIFIER is designed as a modular graph reinforcement learning framework. Different polarization moderation settings are instantiated by modifying the environment transition and reward definition, while the encoder–decoder architecture and the learning procedure remain unchanged. This separation between *decision-making* and *environment dynamics* allows a single trained agent to be applied across a wide range of intervention paradigms.

In particular, the same framework naturally supports the following dimensions of flexibility:

- **Unweighted vs. cost-weighted interventions.** Heterogeneous intervention costs are incorporated by augmenting node features with a cost attribute and by weighting the stepwise reward accordingly. When costs are uniform, the framework reduces to the unweighted setting without any architectural modification.
- **Discrete vs. continuous internal opinions.** PACIFIER operates on both binary opinion assignments (e.g., $\{-1, 1\}$) and continuous-valued internal opinions. Continuous settings are handled through the same graph encoder, while hierarchical, dynamics-aware auxiliary features summarize opinion-induced interaction patterns at multiple thresholds. This enables effective value estimation without assuming linearity or closed-form steady-state solutions.
- **Topology-preserving vs. topology-altering interventions.** Although MI and ME are typically *topology-preserving*, PACIFIER can also accommodate topology-altering interventions such as node removal. In the former case, the graph structure remains invariant and interventions only modify node attributes or impose constraints; in the latter case, the environment transition additionally updates the graph itself. In both settings, the agent continues to operate on the evolving state representation using the same encoder–decoder policy.
- **FJ-model variants, including non-analytic nonlinear dynamics (e.g., biased assimilation).** PACIFIER is agnostic to the specific analytical form of the underlying opinion dynamics. Any FJ-consistent variant—including nonlinear extensions such as biased assimilation that typically admit no closed-form steady state—can be incorporated by modifying only the environment transition and polarization evaluation, while keeping the same encoder–decoder architecture and learning procedure unchanged.

Overall, this modularity allows PACIFIER to serve as a unified learning-based intervention framework for a broad class of polarization moderation problems, spanning different opinion representations, intervention mechanisms, and dynamical models within the Friedkin–Johnsen paradigm and beyond.

5 Experiments

In this section, we evaluate the proposed method on real-world social network datasets with explicit opposing camps. Our experiments are designed to answer the following questions: (i) whether the proposed approach can effectively moderate polarization in realistic network settings, and (ii) how its performance compares to baseline strategies under the same intervention budget. We begin by describing the datasets used in our evaluation, followed by the experimental setup, baselines, and evaluation metrics.

5.1 Datasets

All datasets used in our experiments are derived from the benchmark collection introduced by Garimella et al. [13], which provides topic-induced Twitter interaction graphs together with a two-camp partition for each topic. We start from the complete set of topic graphs released in that work and perform a preliminary filtering step to ensure structural validity and consistency for subsequent analysis.

Specifically, we exclude graphs that (i) contain self-loops, or (ii) do not form a single connected component. These conditions are required to guarantee that polarization measures and intervention dynamics are well-defined over the entire graph and are not dominated by isolated nodes or disconnected subgraphs. No filtering is performed based on polarization level or any algorithmic outcome at this stage.

After this structural filtering, we retain 31 topic graphs. For each retained graph, we compute a comprehensive set of structural and polarization-related statistics, including the number of nodes and edges, the sizes of the two camps, the average degree, the initial polarization, the cross-camp edge ratio, as well as the average degrees within each camp. A

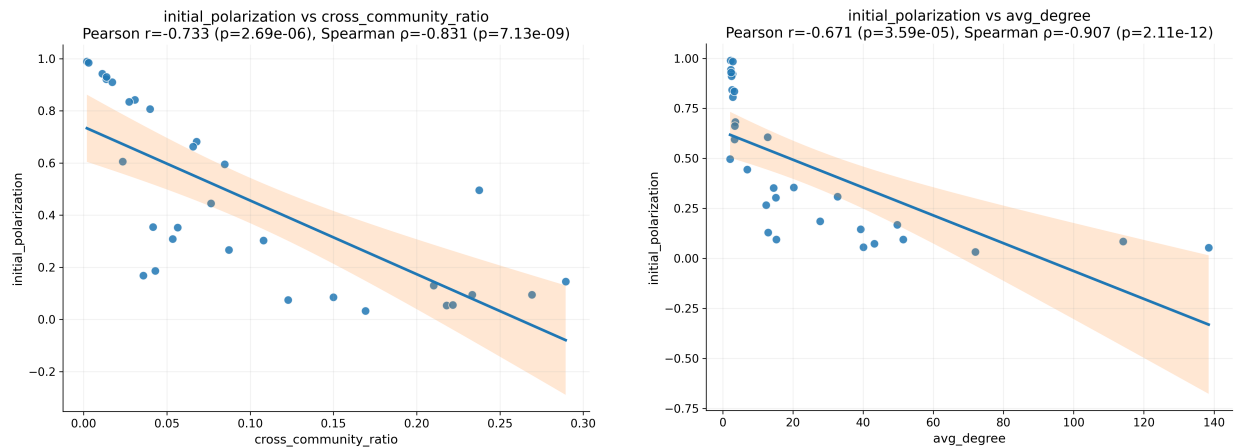
Table 1: Basic statistics of the real-world topic graphs after structural filtering. $|V|$ and $|E|$ denote the number of nodes and edges. $|V^+|$ and $|V^-|$ denote the sizes of the two opposing camps. $\bar{d} = 2|E|/|V|$ is the average degree. $\pi(\mathbf{z}^{(0)})$ is the initial polarization, and ρ_{\pm} denotes the cross-camp edge ratio. \bar{d}^+ and \bar{d}^- are the average degrees of nodes in the positive and negative camps, respectively.

Dataset	$ V $	$ E $	$ V^+ $	$ V^- $	\bar{d}	$\pi(\mathbf{z}^{(0)})$	ρ_{\pm}	\bar{d}^+	\bar{d}^-
follow_russia_march	1189	16471	612	577	27.706	0.186	0.043	30.828	24.393
follow_baltimore	1441	28291	742	699	39.266	0.145	0.289	57.324	20.097
follow_indiasdaughter	1542	9480	748	794	12.296	0.266	0.087	11.583	12.967
follow_gunsense	1821	103840	884	937	114.047	0.085	0.150	86.482	140.053
follow_germanwings	2111	7329	1087	1024	6.944	0.445	0.076	6.307	7.619
follow_ultralive	2113	16070	1088	1025	15.211	0.095	0.233	19.089	11.094
follow_nemtsov	2156	46529	1046	1110	43.162	0.074	0.123	31.801	53.869
follow_mothersday	2225	14160	1145	1080	12.728	0.606	0.023	13.515	11.894
follow_onedirection	3151	20275	1622	1529	12.869	0.130	0.210	15.482	10.097
follow_ukraine	3383	84035	1642	1741	49.681	0.169	0.036	38.452	60.271
follow_ff	3899	63672	1892	2007	32.661	0.308	0.053	38.958	26.725
follow_nepal	4242	42833	2111	2131	20.195	0.354	0.042	24.500	15.930
follow_netanyahu	4292	297136	2208	2084	138.460	0.053	0.218	197.276	76.145
follow_jurassicworld	4395	31802	2262	2133	14.472	0.353	0.056	13.540	15.460
follow_sxsw	4558	91356	2212	2346	40.086	0.056	0.222	35.411	44.494
follow_beefban	799	6026	411	388	15.084	0.303	0.108	22.470	7.260
follow_indiana	946	24328	459	487	51.433	0.094	0.269	27.941	73.575
follow_leadersdebate	9566	344088	4643	4923	71.940	0.032	0.169	49.798	92.822
retweet_wcw	10674	11809	5379	5295	2.213	0.990	0.002	2.341	2.083
retweet_onedirection	15292	26819	7467	7825	3.508	0.682	0.068	3.224	3.778
retweet_mothersday	155599	176915	77799	77800	2.274	0.943	0.011	2.224	2.324
retweet_russia_march	2134	2951	1089	1045	2.766	0.922	0.014	2.826	2.702
retweet_leadersdebate	25983	44174	12726	13257	3.400	0.663	0.066	3.081	3.707
retweet_jurassicworld	26407	32515	13275	13132	2.463	0.911	0.017	2.601	2.323
retweet_germanwings	29763	39075	15142	14621	2.626	0.843	0.031	2.697	2.552
retweet_nepal	40579	57544	19779	20800	2.836	0.807	0.040	2.389	3.261
retweet_nationalkissingday	4638	4816	2250	2388	2.077	0.496	0.238	1.651	2.478
retweet_ff	5401	7646	2621	2780	2.831	0.984	0.003	2.205	3.422
retweet_gunsense	7106	11483	3647	3459	3.232	0.835	0.027	3.468	2.983
retweet_ultralive	9261	15544	4665	4596	3.357	0.596	0.085	2.760	3.962
retweet_sxsw	9304	11003	4519	4785	2.365	0.930	0.014	2.227	2.496

summary of these statistics is reported in Table 1, which provides an overview of the scale, structural diversity, and polarization characteristics of the datasets used in our experiments.

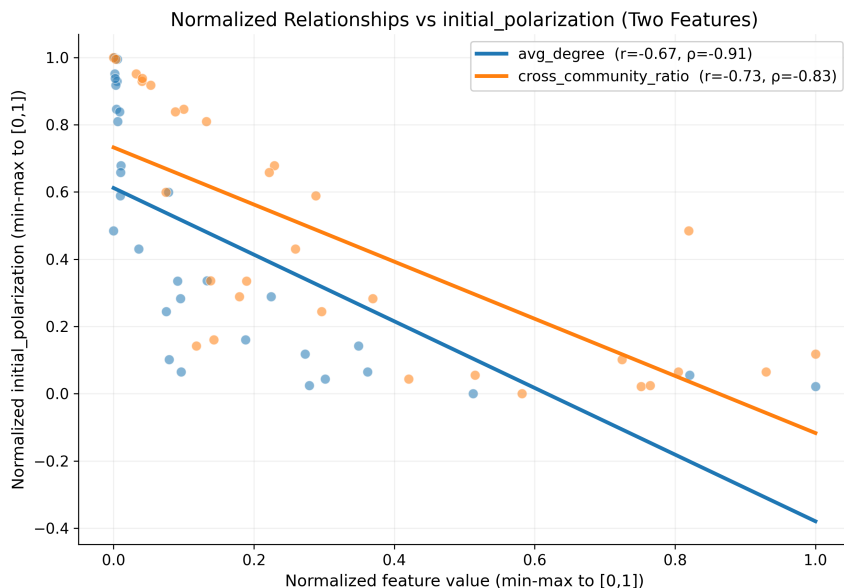
Dataset-level correlation analysis. Beyond the basic statistics in Table 1, we further examine how the initial polarization varies with two intuitive structural indicators across the 31 topic graphs: the average degree \bar{d} and the cross-camp edge ratio ρ_{\pm} . Figures 1a and 1b show clear negative associations between the initial polarization $\pi(\mathbf{z}^{(0)})$ and these two indicators. In particular, the relationship between $\pi(\mathbf{z}^{(0)})$ and the cross-camp edge ratio ρ_{\pm} is strongly negative (Pearson $r = -0.733$, $p = 2.69 \times 10^{-6}$; Spearman $\rho = -0.831$, $p = 7.13 \times 10^{-9}$), indicating that graphs with stronger cross-camp exposure tend to exhibit substantially lower initial polarization. This observation is consistent with the echo-chamber interpretation of polarization: increasing cross-group connectivity weakens segregation and reduces the extent to which opinions align with community boundaries.

Similarly, $\pi(\mathbf{z}^{(0)})$ also decreases with the average degree \bar{d} (Pearson $r = -0.671$, $p = 3.59 \times 10^{-5}$; Spearman $\rho = -0.907$, $p = 2.11 \times 10^{-12}$), suggesting a highly monotonic trend that denser topic graphs are generally less polarized. To facilitate a direct comparison between the two features despite different scales, Figure 1c overlays their min-max normalized relationships. Both features exhibit consistent decreasing trends with polarization, while ρ_{\pm} provides a particularly direct proxy for cross-camp mixing. We emphasize that these results are descriptive correlations across datasets rather than causal claims; nevertheless, they motivate treating cross-camp mixing and connectivity as informative global signals for characterizing polarization regimes in our experimental benchmark.



(a) Cross-camp edge ratio ρ_{\pm} vs. initial polarization.

(b) Average degree \bar{d} vs. initial polarization.



(c) Min-max normalized comparison of \bar{d} and ρ_{\pm} .

Figure 1: Dataset-level relationships between initial polarization $\pi(\mathbf{z}^{(0)})$ and two structural indicators across the 31 topic graphs. Higher cross-camp mixing (larger ρ_{\pm}) and higher connectivity (larger \bar{d}) are associated with lower initial polarization. Pearson and Spearman statistics are reported in the plot titles.

Dataset filtering by initial polarization. While Table 1 summarizes all 31 structurally valid topic graphs, our main experiments further focus on instances with sufficiently strong *initial* polarization. This additional filtering is motivated by two considerations. First, when the initial polarization is very small, the achievable reduction under any intervention budget is limited, which yields weak reward signals and makes reinforcement-learning-based methods difficult to train and evaluate fairly. Second, we aim to select a threshold that retains the majority of genuinely polarized scenarios while excluding graphs that are clearly weakly polarized. Consistent with the dataset-level correlation analysis in Fig. 1a–1c, higher initial polarization tends to coincide with more pronounced echo-chamber structure (i.e., lower cross-camp exposure ρ_{\pm} and typically lower overall connectivity), so focusing on sufficiently polarized instances also emphasizes regimes where echo chambers are structurally clearer.

To make the filtering criterion comparable across datasets, we evaluate the initial polarization under the canonical extreme two-camp configuration, i.e., assigning internal opinions as $s_i \in \{-1, +1\}$ according to the provided two-camp partition (with -1 for one camp and $+1$ for the other), and computing the corresponding settled opinions and initial

Table 2: Datasets retained after polarization-based filtering ($\pi(\mathbf{z}^{(0)}) > 0.4$), sorted by number of nodes.

Dataset	num_nodes	initial_polarization	Dataset	num_nodes	initial_polarization
follow_germanwings	2111	0.444798	retweet_wcw	10674	0.989599
retweet_russia_march	2134	0.922033	retweet_onedirection	15292	0.682127
follow_mothersday	2225	0.605785	retweet_leadersdebate	25983	0.662604
retweet_nationalkissingday	4638	0.496141	retweet_jurassicworld	26407	0.910723
retweet_ff	5401	0.984460	retweet_germanwings	29763	0.842629
retweet_gunsense	7106	0.834818	retweet_nepal	40579	0.807100
retweet_ultralive	9261	0.595510	retweet_mothersday	155599	0.943096
retweet_sxsw	9304	0.930273			

Table 3: Summary statistics (min/mean/max) of key indicators on the filtered benchmark ($\pi(\mathbf{z}^{(0)}) > 0.4$).

Metric	min	mean	max
avg_degree	2.076760	3.707899	12.728100
cross_community_ratio	0.001948	0.047577	0.237542
initial_polarization	0.444798	0.776780	0.989599

polarization $\pi(\mathbf{z}^{(0)})$. We then keep only datasets with $\pi(\mathbf{z}^{(0)}) > 0.4$. This threshold balances coverage and difficulty: it retains most clearly polarized scenarios while excluding weakly polarized graphs where the achievable reduction (and thus the learning signal) is small. The resulting subset constitutes our final experimental benchmark, ensuring that all instances exhibit a clear polarization regime and that interventions produce informative learning signals. The retained datasets (sorted by number of nodes) are summarized in Table 2.

Summary statistics of filtered datasets. To characterize the structural regimes of the filtered benchmark, we additionally report summary statistics (min/mean/max) of three polarization-related indicators computed over the retained topic graphs: the average degree \bar{d} , the cross-camp edge ratio ρ_{\pm} , and the initial polarization $\pi(\mathbf{z}^{(0)})$ under the extreme two-camp configuration. As shown in Table 3, the retained instances exhibit consistently low cross-camp mixing on average (mean $\rho_{\pm} = 0.0476$), while spanning a wide range of connectivity (from sparse graphs with $\bar{d} \approx 2.08$ to denser ones with $\bar{d} \approx 12.73$). Overall, the high mean polarization (0.7768) confirms that this subset concentrates on clearly polarized (echo-chamber-like) regimes where intervention trajectories produce informative reward signals.

Summary statistics of synthetic training/testing graphs. In addition to the real-world benchmark, we also summarize the structural regimes covered by our *synthetic* two-echo-chamber graphs used for offline training and evaluation. Following Sec. 4.2, we generate BA-based two-community graphs with sparse inter-community edges and assign extreme camp opinions (± 1) according to the planted partition. We report, for each size range, the number of generated graphs and the observed value ranges (min–max across graphs) of three indicators: average degree \bar{d} , cross-camp edge ratio ρ_{\pm} , and the resulting initial polarization $\pi(\mathbf{z}^{(0)})$.

As summarized in Table 4, the synthetic graphs span a broad yet consistent regime across all size ranges. Connectivity ranges from sparse to moderately dense graphs (approximately $\bar{d} \in [1.87, 11.66]$ across all ranges), while cross-camp exposure remains low by construction (typically $\rho_{\pm} \in [0.00, 0.17]$), producing strongly polarized initial states with $\pi(\mathbf{z}^{(0)})$ often close to 1.0 and ranging roughly from 0.06 to 1.00 depending on the sampled inter-camp edges. Importantly, these ranges cover the regimes emphasized by our real-world filtered benchmark (Table 3), where echo-chamber structure corresponds to low ρ_{\pm} and higher polarization. Moreover, the per-range statistics are highly stable as graph size increases from 30–50 up to 400–500 nodes: the min–max intervals of \bar{d} , ρ_{\pm} , and $\pi(\mathbf{z}^{(0)})$ remain comparable across ranges. This indicates that these three indicators are largely *scale-insensitive* in our synthetic generator—they characterize the echo-chamber *regime* (connectivity and mixing) rather than the absolute graph size—which is desirable for inductive learning and evaluation across sizes. In particular, the training range (30–50) already overlaps the global synthetic ranges and exhibits the same low-mixing/high-polarization pattern, while larger ranges preserve similar statistics, supporting inductive generalization from small training graphs to larger test graphs.

Table 4: Per-range statistics of synthetic graphs used for training/testing. For each node-size range, we report the number of generated graphs and the min–max range of \bar{d} , ρ_{\pm} , and $\pi(\mathbf{z}^{(0)})$ under the extreme two-camp assignment.

range	n_graphs	avg_degree	cross_community_ratio	initial_polarization
30–50	100	1.87~9.26	0.00~0.17	0.09~1.00
50–100	100	1.92~10.54	0.00~0.17	0.07~1.00
100–200	100	1.98~11.23	0.01~0.16	0.07~0.98
200–300	100	2.01~11.52	0.01~0.16	0.06~0.96
300–400	100	2.07~11.52	0.01~0.17	0.07~0.88
400–500	100	2.01~11.66	0.01~0.16	0.06~0.97

5.2 Visualization Protocol and Evaluation Views

To provide a comprehensive and interpretable evaluation across intervention tasks and datasets, we report results using three complementary visualization views: *per-dataset bar charts*, *heatmap summaries*, and *polarization trajectories*.

(1) Per-dataset bar charts (AUC / ANP summary). For each task and each dataset, we report the accumulated normalized polarization (ANP) (or its AUC-style equivalent) as a single scalar performance metric. Lower values indicate better overall trajectory-aware performance. Bar charts allow direct horizontal comparison between methods on the same dataset, highlighting absolute gains and relative ranking.

(2) Heatmap overview (cross-dataset consistency). To visualize performance consistency across all datasets simultaneously, we present method \times dataset heatmaps. Each cell represents the ANP/AUC score of a method on a dataset. This view emphasizes vertical comparisons (how a method behaves across datasets) and horizontal comparisons (which datasets are intrinsically harder). Heatmaps make it easy to identify systematic advantages rather than isolated wins.

(3) Polarization trajectories (temporal behavior). Since our evaluation metric rewards early and persistent polarization reduction, we additionally visualize full intervention trajectories on representative datasets. Trajectory plots reveal *when* polarization reduction occurs, distinguishing methods that reduce polarization early from those that only improve near the budget limit. Better methods exhibit steeper early-stage decline and maintain lower curves throughout the horizon.

Together, these three views provide complementary perspectives: bar charts summarize final trajectory quality, heatmaps highlight cross-dataset robustness, and trajectories explain the temporal dynamics underlying AUC differences.

5.3 Synthetic Benchmark: Performance across Graph Sizes

We further evaluate PACIFIER on a controlled *synthetic* benchmark to examine generalization across graph sizes and to provide an apples-to-apples comparison with competing methods under identical instance distributions. We generate two-echo-chamber graphs following the procedure in Sec. 4.2, and report results on six node-size ranges: {30–50, 50–100, 100–200, 200–300, 300–400, 400–500}. For each size range, we sample 100 graphs, resulting in 600 test instances in total. We compare PACIFIER against all baselines on four tasks: MI, MI-COST, ME, and ME-COST. In each bar chart, the x-axis corresponds to the node-size range and each bar reports the average score over the 100 graphs in that range (with error bars showing the standard deviation when available).

Discussion. As shown in Fig. 2, the synthetic benchmark reveals three qualitatively different regimes across tasks, which together clarify when long-horizon reinforcement learning is essential and when myopic learning already suffices.

(1) MI (unweighted): PACIFIER matches the linear-model optimum. From Fig. 2a, we observe that on the canonical MI task, both PACIFIER-RL and PACIFIER-Greedy achieve performance nearly indistinguishable from BOMP, the classical model-aware algorithm that explicitly exploits the linear structure of the FJ steady-state solution. Across all graph-size ranges (30–50 up to 400–500), the two PACIFIER variants closely track the BOMP curve and significantly outperform purely structural heuristics such as PageRank, ExtremeExpressed, ExtremeNeighbours, and random selection. This indicates that the learned representation successfully captures the same influence structure that BOMP leverages analytically, despite not using closed-form matrix inversions during deployment. Moreover, the negligible gap between PACIFIER-RL and PACIFIER-Greedy suggests that in this linear, unweighted setting, the

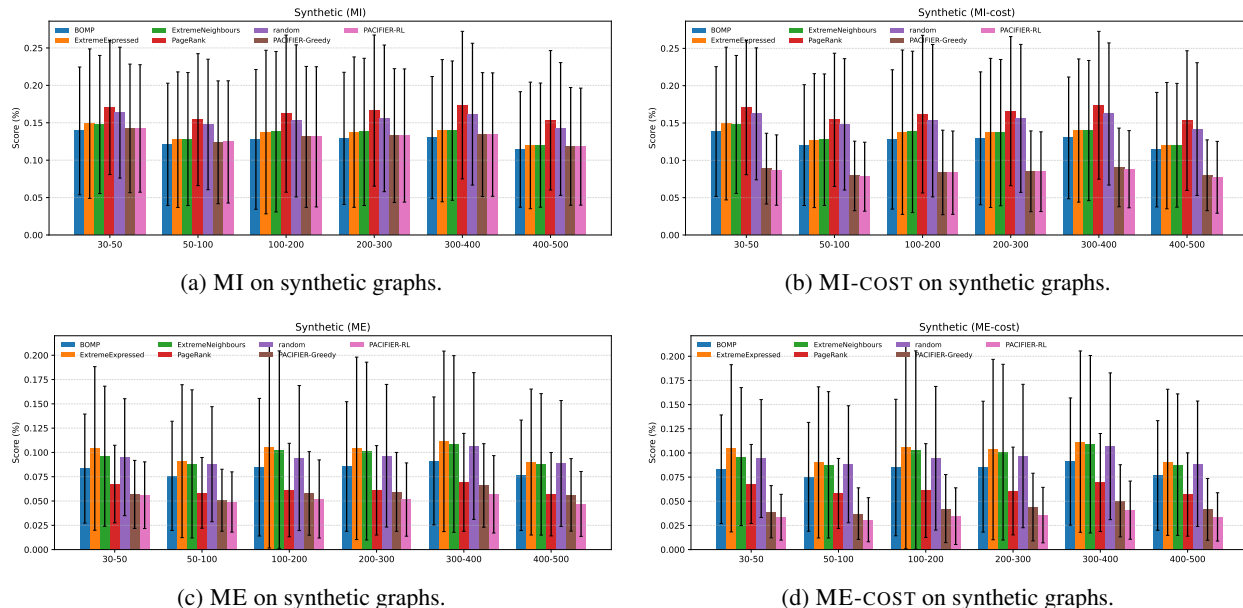


Figure 2: Synthetic benchmark results across six node-size ranges (30–50, 50–100, 100–200, 200–300, 300–400, 400–500), with 100 graphs per range. Bars compare PACIFIER with all baselines on four tasks: MI, MI-COST, ME, and ME-COST. Lower is better if the reported metric is polarization/ANP; higher is better if it is a score (%). (See the main text for the exact metric definition used in these plots.)

immediate polarization-reduction signal is already highly aligned with the long-horizon objective; thus, myopic value estimation is sufficient to approximate near-optimal action ranking.

(2) MI-cost: RL and Greedy remain close, but both dominate heuristics. As illustrated in Fig. 2b, when heterogeneous intervention costs are introduced (MI-COST), both PACIFIER variants continue to substantially outperform classical heuristics. Although BOMP is no longer directly optimal under cost-weighting, **PACIFIER-RL** and **PACIFIER-Greedy** remain very close to each other across all scales, indicating that even with cost-aware trade-offs, the immediate reward remains a strong proxy for long-term utility. Importantly, both variants consistently outperform structural baselines, demonstrating that the encoder–decoder architecture internalizes cost-sensitive influence patterns without relying on linear closed-form solutions.

(3) ME and ME-cost: long-horizon RL becomes essential. In contrast, Fig. 2c and Fig. 2d show that under ME and especially ME-COST, **PACIFIER-RL** decisively outperforms **PACIFIER-Greedy** across all graph sizes. The gap between RL and Greedy is persistent and substantial, while both PACIFIER variants clearly dominate all traditional baselines. This indicates that fixing expressed opinions induces stronger sequential and interaction effects: the benefit of intervening on one node depends critically on how the system re-equilibrates and how future feasible actions are reshaped by previously fixed constraints. Such dependencies cannot be captured by immediate reward regression alone, but are naturally learned through bootstrapped Q-learning. The stability of this RL advantage across graph scales confirms that long-horizon credit assignment is fundamentally important for ME-style interventions rather than being a small-graph artifact.

(4) Scalability and regime-dependent optimality. Across all four subfigures in Fig. 2, performance remains remarkably stable as the graph size increases by an order of magnitude. The relative ordering between methods does not change with scale, demonstrating strong inductive generalization from small training graphs to larger synthetic instances. Collectively, the results illustrate a regime-dependent phenomenon: when the task admits a strong linear analytical structure (as in MI), PACIFIER recovers near-optimal behavior comparable to BOMP; when that structure is weakened by cost heterogeneity or by expressed-opinion constraints (MI-COST, ME, ME-COST), learning-based long-horizon reasoning provides clear and consistent gains.

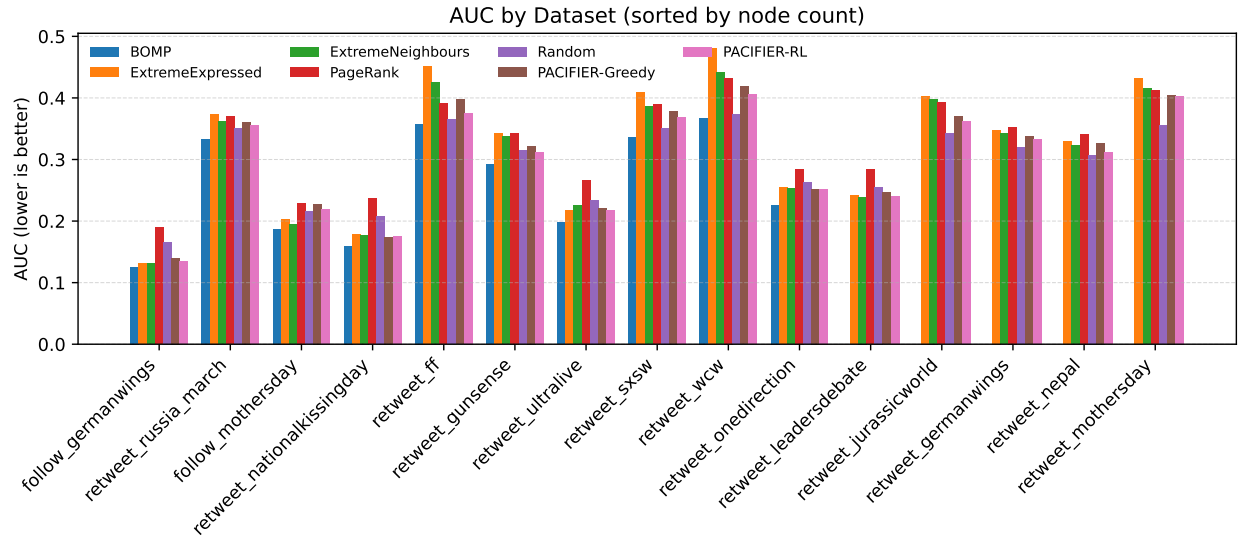


Figure 3: Real datasets (MI): per-dataset bar comparison (lower is better).

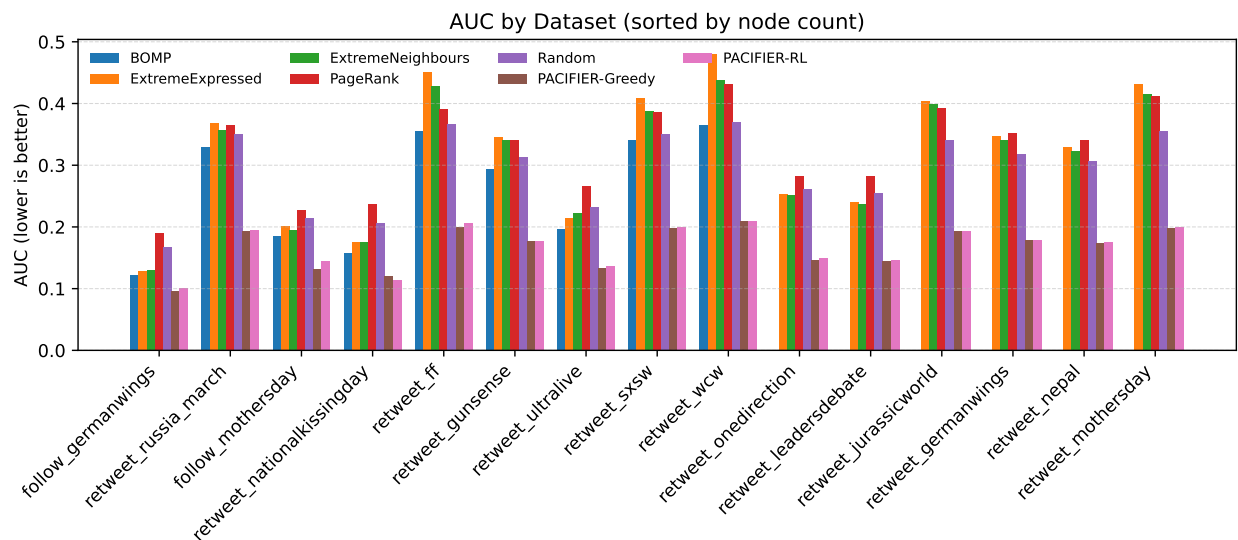


Figure 4: Real datasets (MI-cost): per-dataset bar comparison (lower is better).

5.4 Real-world Datasets (origin)

We report results on the real-world polarized topic graphs described in Sec. 5.1. For each task, we provide: (i) a per-dataset bar chart summarizing the ANP/AUC-style metric, (ii) a heatmap overview across datasets and methods, and (iii) aggregated polarization trajectories.

Per-dataset bar charts. The following bar charts compare **PACIFIER** with all baselines on each dataset. Lower values indicate better trajectory-aware performance (area-under-curve / accumulated metric).

Heatmap overview. Heatmaps provide a compact view of method performance across all datasets, highlighting relative strengths and weaknesses under different intervention settings.

Trajectory curves (representative datasets). To qualitatively illustrate *when* polarization reduction happens along the intervention horizon, we visualize polarization trajectories on **three representative datasets** for each task. Specifically,

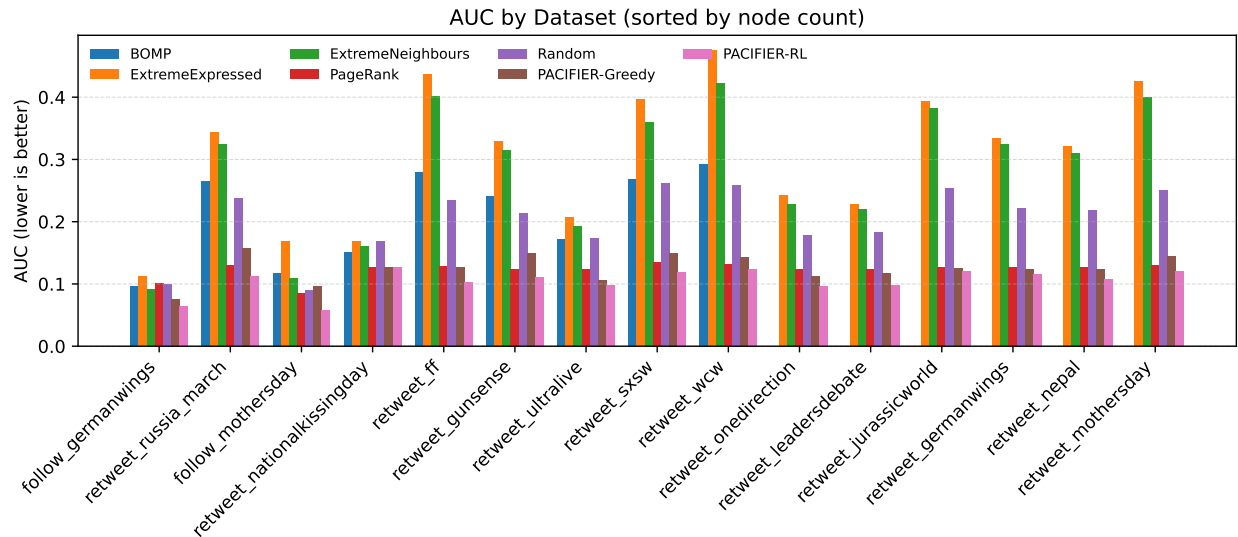


Figure 5: Real datasets (ME): per-dataset bar comparison (lower is better).

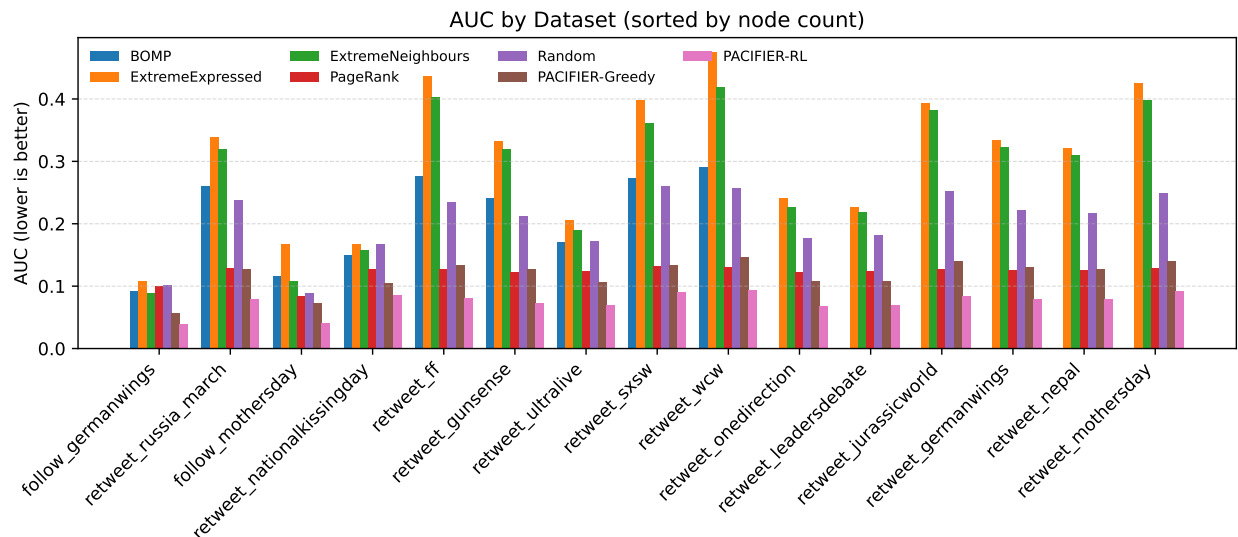


Figure 6: Real datasets (ME-cost): per-dataset bar comparison (lower is better).

we select (i) the dataset with the smallest number of nodes, (ii) the largest dataset whose size is below a threshold (e.g., $n < 20,000$), and (iii) the dataset with the largest number of nodes. This selection covers small/medium/large regimes while keeping the main text concise. The complete set of trajectory plots for all datasets is provided in Appendix.

5.4.1 Discussion

We next analyze the real-world results in detail. For each intervention setting (MI, MI-cost, ME, and ME-cost), we discuss the empirical findings from three complementary perspectives: (i) per-dataset bar comparisons, (ii) heatmap-level performance patterns across datasets, and (iii) representative polarization trajectories that reveal the dynamic evolution of polarization. We examine each task individually and then summarize the broader trends observed across settings.

MI. On the MI setting, PACIFIER does not outperform the strongest non-PACIFIER baselines on the real-world graphs. As shown in Fig. 3, BOMP achieves the lowest accumulated metric on the majority of datasets, with an average AUC of 0.258 compared to 0.298 for PACIFIER-RL and 0.305 for PACIFIER-Greedy. Across all 15 datasets,

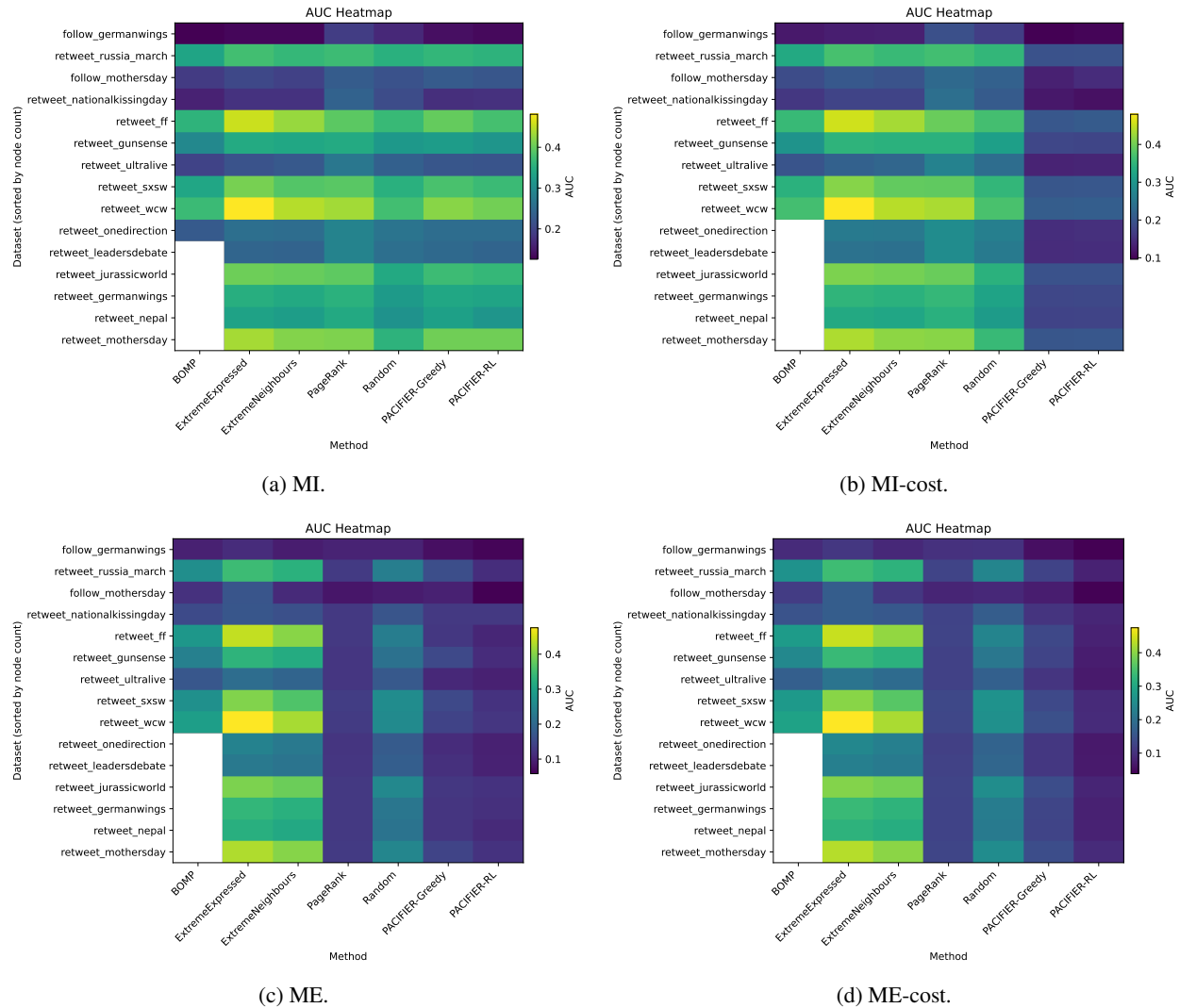


Figure 7: Real datasets (origin): heatmap summaries for MI/MI-cost/ME/ME-cost. Lower is better.

PACIFIER-RL does not achieve the best result on any instance, and the average relative gap to the strongest baseline is approximately 8%, with larger discrepancies observed on some small-scale graphs.

The heatmap in Fig. 7a further confirms this pattern. The advantage of classical structural heuristics such as BOMP and ExtremeNeighbours is consistent across small, medium, and large graphs. Although the performance gap slightly narrows as the graph size increases (e.g., on large retweet networks), PACIFIER remains systematically behind the best-performing baseline in all size regimes.

The representative trajectory plots in Fig. 8 provide additional insight into this behavior. On small graphs (e.g., *follow_germanwings*), PACIFIER reduces polarization more slowly in the early intervention stages and fails to catch up later, leading to a consistently higher trajectory. On medium and large graphs (e.g., *retweet_onedirection* and *retweet_mothersday*), PACIFIER follows a trajectory that remains above the strongest baseline throughout the horizon, indicating that the gap is not due to late-stage instability but rather a persistent structural disadvantage. Overall, under the MI objective on real-world graphs, classical heuristics appear better aligned with the polarization structure than the learned PACIFIER strategy.

MI-cost. The picture changes dramatically under the cost-aware MI setting. As shown in Fig. 4, both PACIFIER-RL and PACIFIER-Greedy consistently achieve the lowest accumulated metric across all 15 datasets. PACIFIER-RL improves over the strongest non-PACIFIER baseline on every dataset, with a mean relative gain of approximately 37%

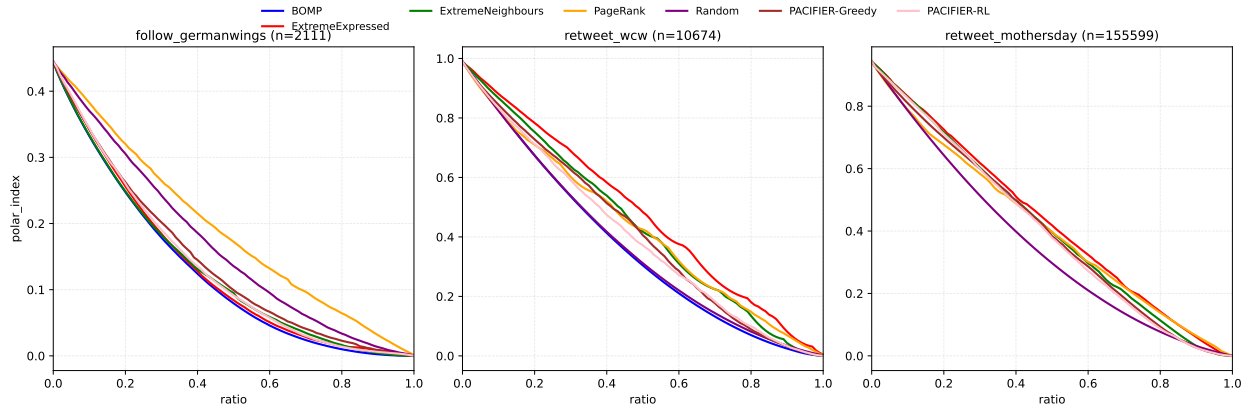


Figure 8: Real datasets (MI): polarization trajectories on three representative datasets (small / medium / large by node count). Lower and earlier is better. Full trajectories for all datasets are in Appendix.

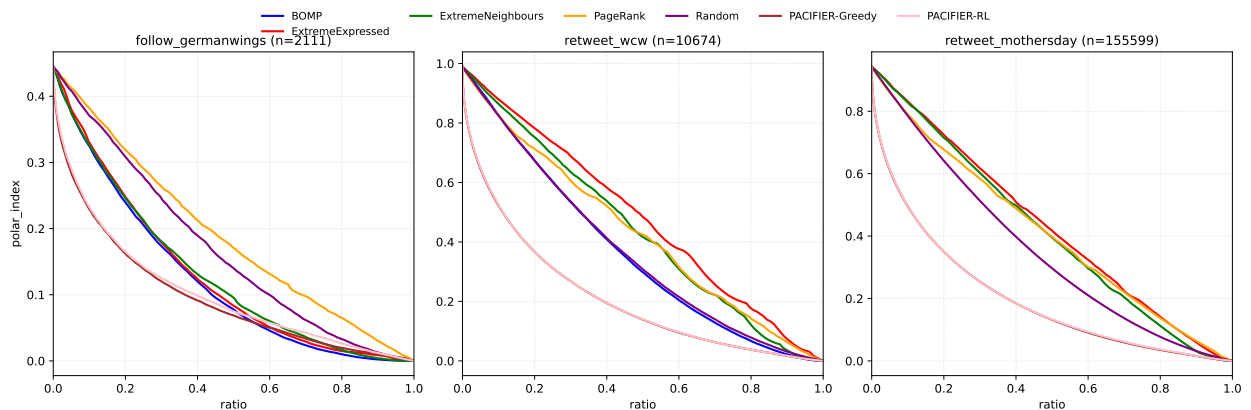


Figure 9: Real datasets (MI-cost): polarization trajectories on three representative datasets (small / medium / large by node count). Lower and earlier is better. Full trajectories for all datasets are in Appendix.

(median 41%), while PACIFIER-Greedy achieves a comparable mean improvement of about 38%. This represents a complete reversal of the trend observed in the cost-free MI setting.

The heatmap in Fig. 7b further highlights the stability of this advantage. Unlike the MI case, where classical heuristics dominate, PACIFIER uniformly outperforms all baselines across small, medium, and large graphs. Moreover, the relative improvement increases with graph size: the average gain is around 27% on small graphs, rises to nearly 40% on medium graphs, and exceeds 42% on large-scale networks. This clear scalability pattern suggests that PACIFIER is particularly effective when intervention decisions must be made under budget constraints in large real-world graphs.

The representative trajectory plots in Fig. 9 provide insight into the source of this improvement. On small graphs (e.g., *follow_germanwings*), PACIFIER reduces polarization more aggressively from the early stages, resulting in a visibly lower trajectory throughout the intervention horizon. On medium and large graphs (e.g., *retweet_onedirection* and *retweet_mothersday*), the gap becomes even more pronounced: PACIFIER maintains a substantially lower trajectory at nearly every step, rather than merely converging to a better final value. This indicates that the advantage stems from consistently better budget allocation decisions, leading to sustained polarization suppression over time.

ME. Under the ME objective, PACIFIER-RL consistently achieves the best performance across all real-world datasets. As illustrated in Fig. 5, PACIFIER-RL attains the lowest accumulated metric on all 15 datasets, with an average AUC of 0.105, outperforming the strongest non-PACIFIER baseline (typically PageRank) by approximately 15% on average. The improvement is particularly pronounced on certain small graphs (up to 31% relative gain), while even on the most challenging instances the advantage remains positive.

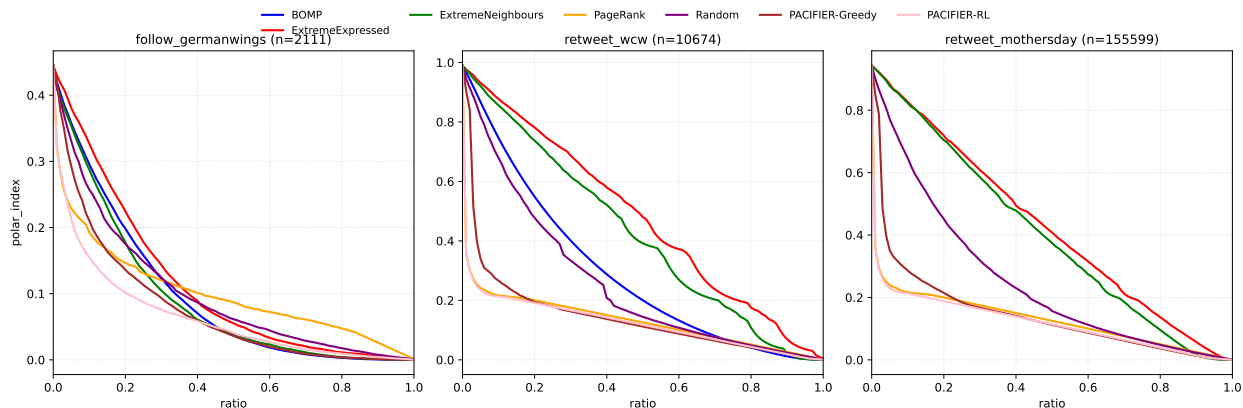


Figure 10: Real datasets (ME): polarization trajectories on three representative datasets (small / medium / large by node count). Lower and earlier is better. Full trajectories for all datasets are in Appendix.

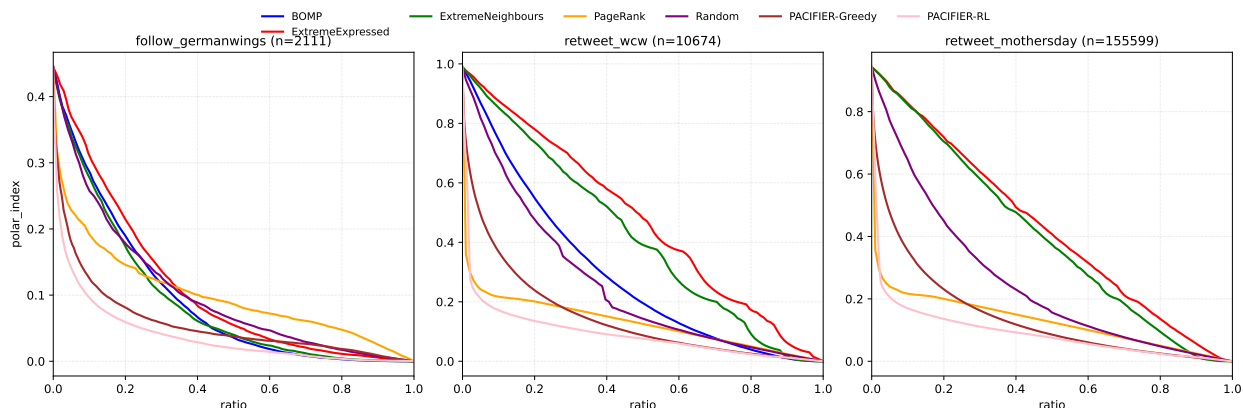


Figure 11: Real datasets (ME-cost): polarization trajectories on three representative datasets (small / medium / large by node count). Lower and earlier is better. Full trajectories for all datasets are in Appendix.

The heatmap in Fig. 7c confirms that this dominance is stable across scales. PACIFIER-RL achieves a 100% win rate in small-, medium-, and large-scale regimes, with mean relative gains of roughly 19%, 14%, and 13%, respectively. Although the improvement magnitude slightly decreases as graph size grows, the method remains consistently superior across all size buckets. In contrast, PACIFIER-Greedy exhibits noticeably less stability, winning only 60% of datasets overall and showing performance degradation on several small and medium graphs, highlighting the benefit of the reinforcement learning component.

The representative trajectory plots in Fig. 10 further clarify the source of the improvement. On small graphs (e.g., *follow_germanwings*), PACIFIER-RL rapidly suppresses polarization in early stages, creating a clear separation from structural heuristics. On medium graphs (e.g., *retweet_onedirection*), the advantage is maintained steadily across the entire horizon. Even on very large graphs (e.g., *retweet_mothersday*), PACIFIER-RL preserves a consistently lower trajectory than PageRank, whereas PACIFIER-Greedy occasionally loses its advantage. Overall, under the ME objective, the learned RL policy demonstrates strong and robust generalization on real-world networks.

ME-cost. Under the cost-aware ME objective, PACIFIER-RL achieves the strongest overall performance among all methods. As shown in Fig. 6, PACIFIER-RL attains the lowest accumulated metric on all 15 datasets, with an average AUC of 0.075, substantially outperforming the strongest non-PACIFIER baseline by approximately 39% on average. The relative gain remains positive on every dataset, with improvements ranging from about 29% to nearly 57%, indicating highly consistent dominance under budget constraints.

The heatmap in Fig. 7d further demonstrates the robustness of this advantage. PACIFIER-RL achieves a 100% win rate across small-, medium-, and large-scale graphs, with mean improvements of roughly 45% on small graphs, 36% on medium graphs, and 38% on large graphs. Unlike the cost-free ME setting, where the improvement magnitude slightly

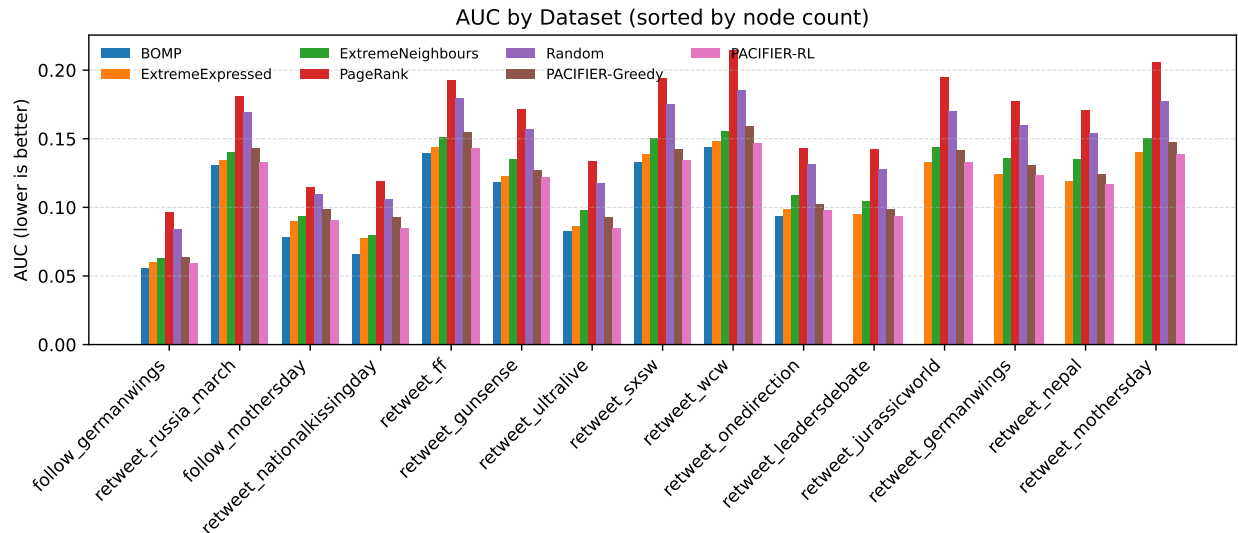


Figure 12: Real datasets (MI-continuous): AUC summary by dataset (lower is better).

decreases with scale, the cost-aware formulation preserves a strong and stable advantage across all regimes. In contrast, PACIFIER-Greedy exhibits considerable instability, achieving only partial wins (approximately 47% overall) and even negative improvements on several medium and large datasets, highlighting the importance of the learned RL policy in budget-sensitive scenarios.

The representative trajectory plots in Fig. 11 illustrate the dynamic source of this superiority. On small graphs (e.g., *follow_germanwings*), PACIFIER-RL dramatically lowers polarization from the earliest intervention stages, creating a large and persistent separation from structural heuristics. On medium and large graphs (e.g., *retweet_onedirection* and *retweet_mothersday*), the RL policy maintains a consistently lower trajectory throughout the horizon, rather than merely achieving a better final value. This sustained gap suggests that PACIFIER-RL effectively prioritizes influential nodes under budget constraints, resulting in systematically improved polarization mitigation over time.

5.5 Real Datasets: Extended Settings

We further evaluate PACIFIER under several FJ-consistent extensions on real-world topic graphs, including continuous-valued opinions, nonlinear biased-assimilation dynamics, and topology-altering intervention (node removal). We present (i) per-dataset AUC-style summary bars, (ii) cross-dataset method \times dataset heatmaps, and (iii) *representative* trajectory curves (three datasets) to illustrate *when* polarization is reduced. Full trajectory plots for all datasets are deferred to the Appendix.

AUC summary (bar; by dataset). The bar plots summarize each method’s performance on every real dataset under the same budget, where lower is better. Since the plots are wide, we place one bar chart per line.

Discussion (bar). Across these extended settings, PACIFIER remains competitive and typically achieves the best or near-best AUC on the majority of datasets, indicating robust generalization beyond the base linear FJ setting and beyond topology-preserving interventions.

Per-dataset comparison (heatmap). We additionally visualize method performance across datasets using heatmaps. These heatmaps highlight which datasets are consistently easy/hard and whether a method’s gains are uniform or dataset-dependent.

Discussion (heatmap). The heatmaps suggest PACIFIER’s gains are broadly distributed across datasets rather than driven by a small subset, while any occasional regressions tend to be localized to a few datasets, indicating robust cross-dataset performance.

Trajectory curves (representative; three datasets). To visualize the *timing* of polarization reduction, we show representative trajectories on three datasets (chosen to cover small/medium/large graph sizes). Better methods reduce

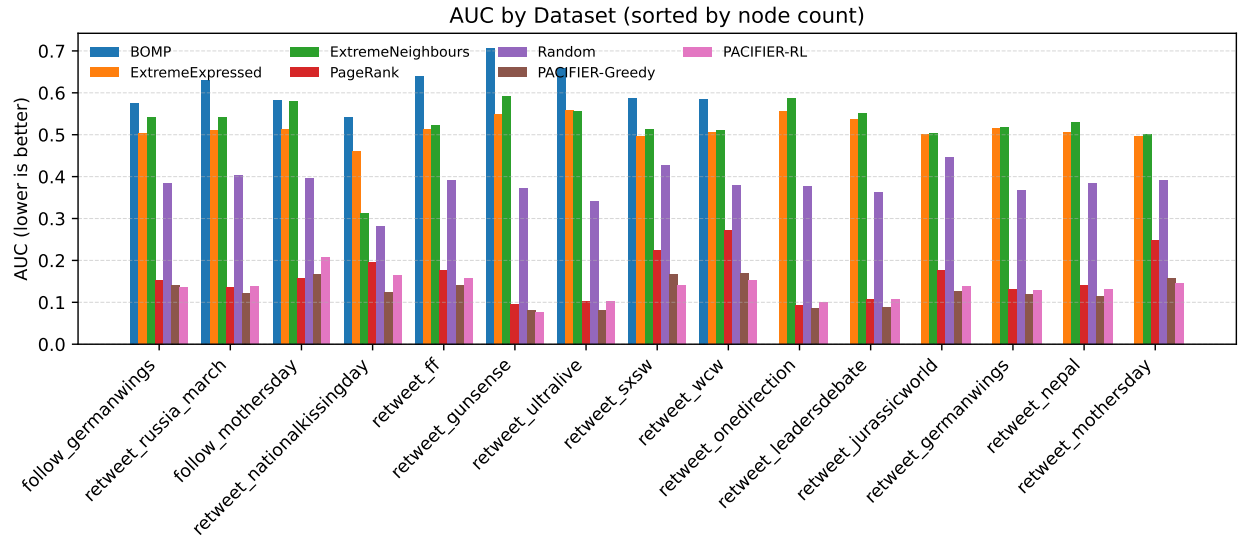


Figure 13: Real datasets (MI-bias_assmilate): AUC summary by dataset (lower is better).

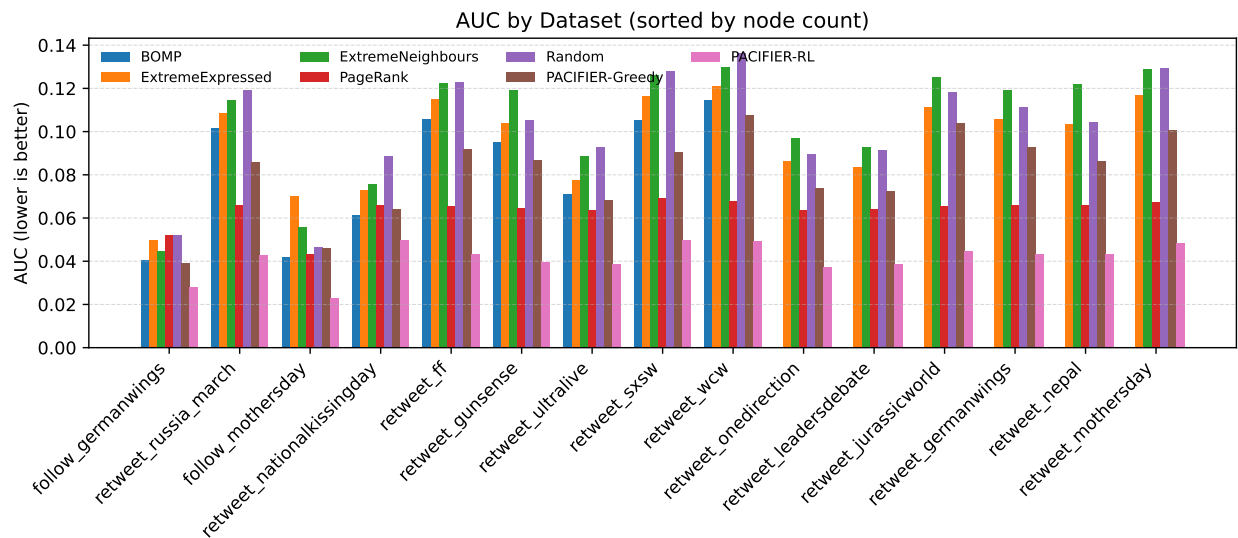


Figure 14: Real datasets (ME-continuous): AUC summary by dataset (lower is better).

polarization earlier and keep it lower throughout the horizon. The complete set of per-dataset trajectory plots is provided in the Appendix.

5.5.1 Discussion

We next analyze the results under the extended FJ-consistent settings. For each variant (MI-continuous, MI-bias_assmilate, ME-continuous, and node_removal), we examine the empirical behavior from three complementary perspectives: (i) per-dataset AUC comparisons, (ii) cross-dataset heatmap patterns, and (iii) representative polarization trajectories that reveal the temporal dynamics of intervention. We discuss each setting individually and then summarize the broader robustness patterns across these extended dynamics.

MI-continuous. Under continuous-valued opinion dynamics, the performance landscape changes substantially compared with the discrete MI setting. From the per-dataset AUC bars (Fig. 12), **BOMP** achieves the lowest average AUC (0.104), while **PACIFIER-RL** ranks second overall (avg. 0.114) and **PACIFIER-Greedy** follows closely behind.

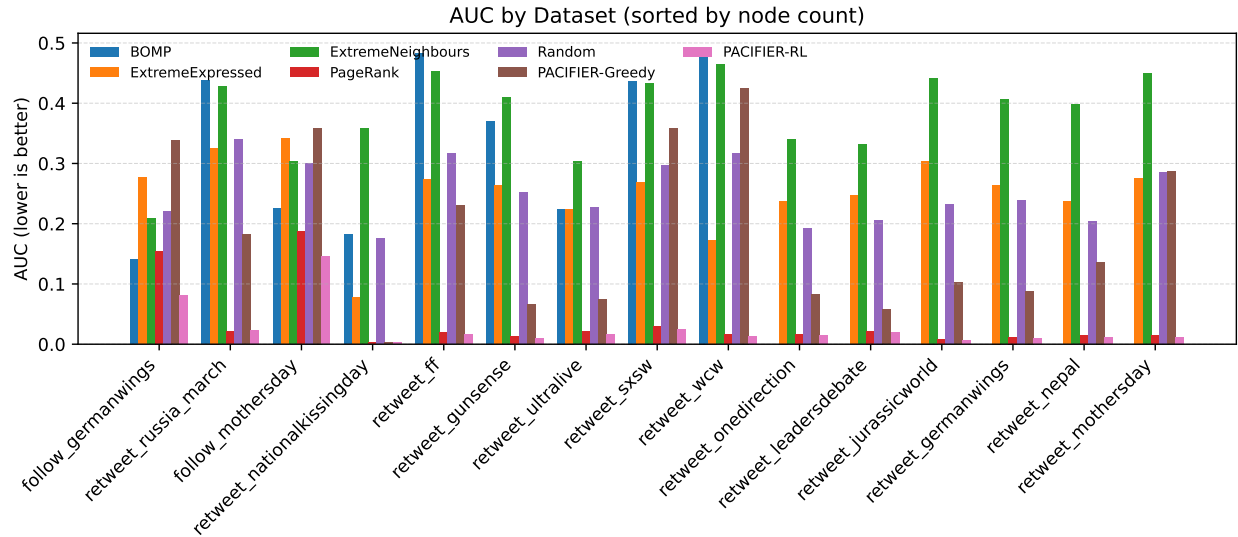
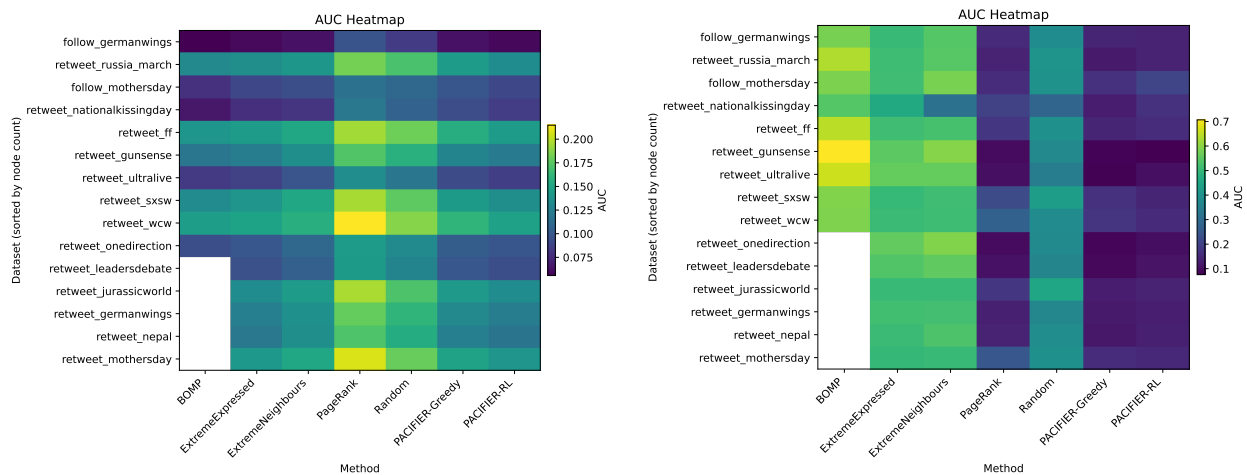


Figure 15: Real datasets (node_removal): AUC summary by dataset (lower is better).



(a) MI-continuous.

(b) MI-bias_assmilate.

Figure 16: Real datasets (extended): AUC heatmaps across datasets (lower is better).

Across all 15 datasets, PACIFIER-RL outperforms the best non-PACIFIER baseline on 5 datasets (33% win rate), whereas PACIFIER-Greedy does not achieve wins against the strongest baseline.

The heatmap (Fig. 16a) reveals a clear size-dependent pattern. On small and mid-sized graphs (up to 15k nodes), BOMP remains consistently dominant, and both PACIFIER variants show a mild but systematic gap. However, on large graphs (> 15,000 nodes), PACIFIER-RL becomes competitive and wins on 5 out of 6 datasets, with a slight positive average improvement ($\text{imp_mean} \approx 0.2\%$). This suggests that when graph scale increases and analytical structure becomes harder to exploit precisely, the learned policy begins to match or slightly exceed classical influence-based heuristics.

The representative trajectory curves (Fig. 18) further clarify this behavior. On small datasets (e.g., *follow_germanwings*), BOMP reduces polarization slightly earlier and maintains the lowest curve. On medium-scale datasets, PACIFIER-RL closely tracks BOMP but does not surpass it. On the largest dataset (*retweet_mothersday*), PACIFIER-RL achieves the best final AUC and maintains a marginally lower trajectory than all baselines, while PACIFIER-Greedy remains slightly behind.

Overall, MI-continuous exhibits a regime where analytical linear structure still provides a strong advantage on small graphs, but PACIFIER-RL demonstrates increasing competitiveness as scale grows. The gap between RL and Greedy

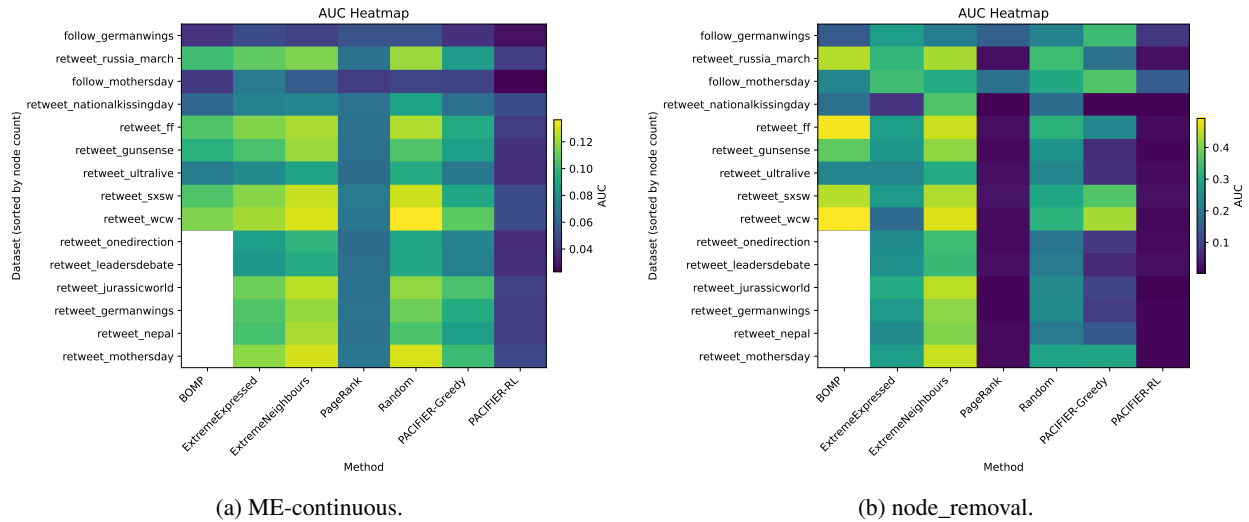


Figure 17: Real datasets (extended): AUC heatmaps across datasets (lower is better).

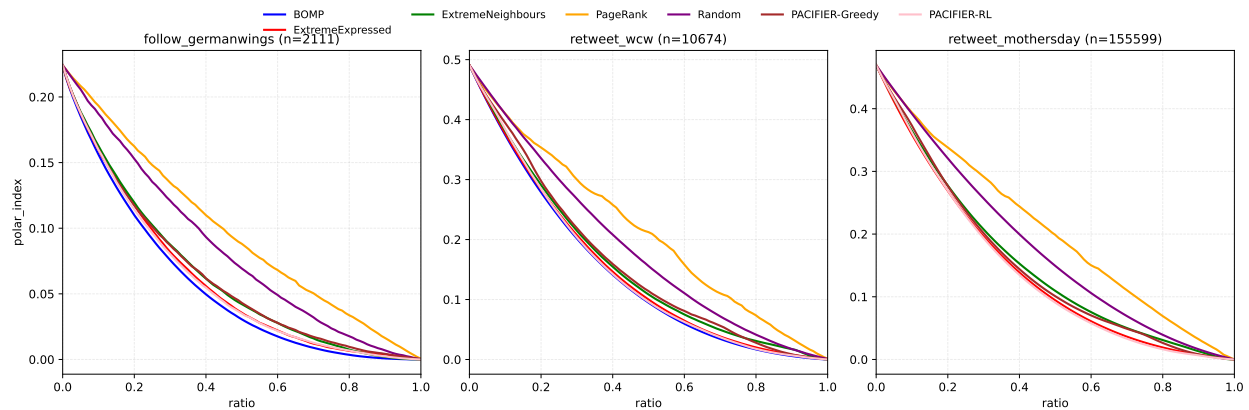


Figure 18: Real datasets (MI-continuous): representative polarization trajectories on three datasets (lower and earlier is better). Full trajectories are deferred to the Appendix.

indicates that even under continuous opinions, long-horizon credit assignment provides moderate benefits, though not as decisively as in the ME-style tasks.

MI-bias assimilate. Under nonlinear biased-assimilation dynamics, the relative ordering of methods changes markedly compared with the continuous linear case. From the per-dataset AUC bars (Fig. 13), both **PACIFIER-Greedy** (avg. 0.126) and **PACIFIER-RL** (avg. 0.135) substantially outperform all classical baselines, with PageRank being the strongest non-PACIFIER competitor (avg. 0.161). In contrast, BOMP—designed for linear steady-state structure—degrades significantly under biased assimilation.

Per-dataset comparisons show that **PACIFIER-Greedy** wins on 14 out of 15 datasets (93% win rate) against the best non-PACIFIER baseline, achieving an average relative improvement of approximately 19%. **PACIFIER-RL** also performs strongly (73% win rate, mean improvement $\approx 11\%$), though slightly behind the Greedy variant in aggregate. The heatmap (Fig. 16b) confirms that these gains are broadly distributed across datasets rather than concentrated on a few outliers.

A scale-aware pattern also emerges. On mid-sized graphs (5k–15k nodes), both PACIFIER variants achieve a 100% win rate and large improvement margins (mean $\approx 22\text{--}24\%$). On large graphs ($> 15\text{k}$ nodes), PACIFIER-Greedy remains consistently dominant (6/6 wins), while PACIFIER-RL remains competitive but slightly less stable. This suggests that under nonlinear opinion dynamics, immediate polarization reduction signals align well with long-term objectives, making myopic value estimation particularly effective.

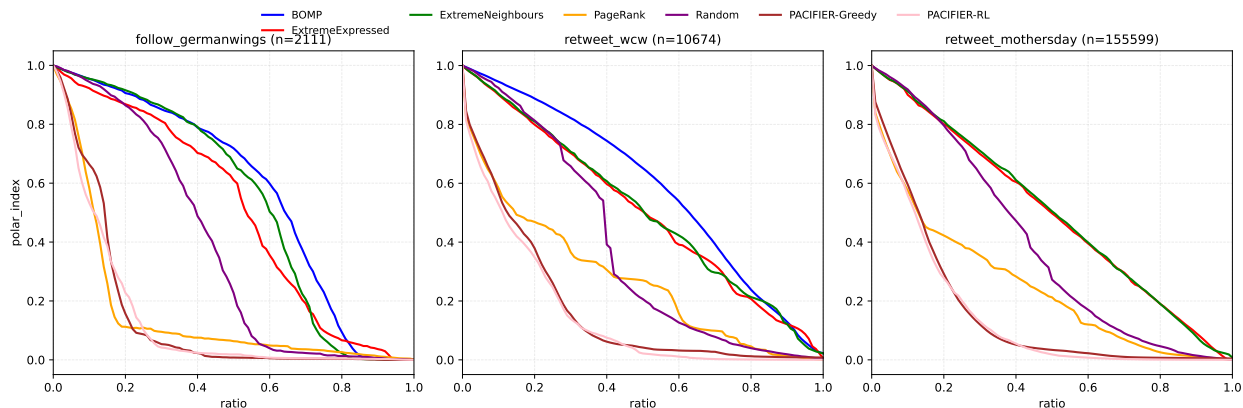


Figure 19: Real datasets (MI-bias_assmlate): representative polarization trajectories on three datasets (lower and earlier is better). Full trajectories are deferred to the Appendix.

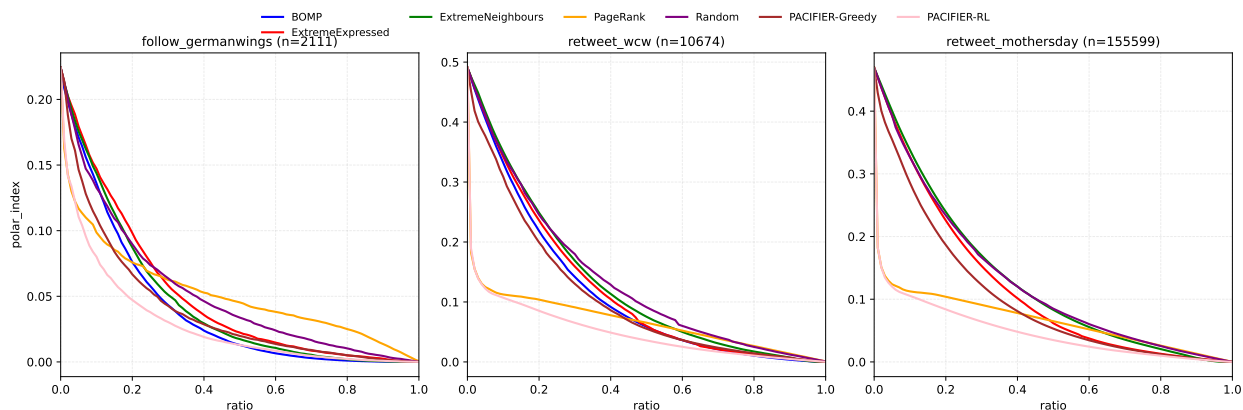


Figure 20: Real datasets (ME-continuous): representative polarization trajectories on three datasets (lower and earlier is better). Full trajectories are deferred to the Appendix.

The representative trajectory plots (Fig. 19) further illustrate this regime. On small graphs (e.g., *follow_germanwings*), both PACIFIER variants reduce polarization earlier than PageRank. On medium graphs, PACIFIER-Greedy often attains the lowest curve. On large graphs (e.g., *retweet_mothersday*), both variants substantially outperform classical baselines, with clear early-stage and sustained advantages.

Overall, MI-bias_assmlate demonstrates a setting where learning-based policies decisively outperform analytical linear-structure methods. Interestingly, the Greedy variant slightly surpasses RL on average, indicating that under biased assimilation, short-horizon gains already capture much of the effective intervention signal.

ME-continuous. Under continuous expressed-opinion intervention (ME-continuous), a clear separation emerges between long-horizon reinforcement learning and myopic estimation. From the per-dataset AUC bars (Fig. 14), **PACIFIER-RL** achieves the best overall performance with a substantial margin (avg. 0.041), while the strongest classical baseline, PageRank, remains significantly higher (avg. 0.063). In contrast, **PACIFIER-Greedy** (avg. 0.081) performs similarly to BOMP and does not exhibit consistent gains.

Per-dataset comparisons highlight the dominance of RL: PACIFIER-RL wins on *all 15 datasets* (100% win rate), with an average relative improvement of approximately 34% over the best non-PACIFIER baseline. The improvement is stable across all scale buckets: small, mid, and large graphs each show consistent 30–35% average gains. By contrast, PACIFIER-Greedy wins only once (1/15 datasets), and its average improvement is strongly negative, particularly on mid- and large-scale graphs.

The heatmap (Fig. 17a) confirms that RL’s advantage is not driven by a small subset of datasets, but is uniformly distributed across scales. This pattern indicates that under ME-style dynamics, sequential dependency and long-horizon

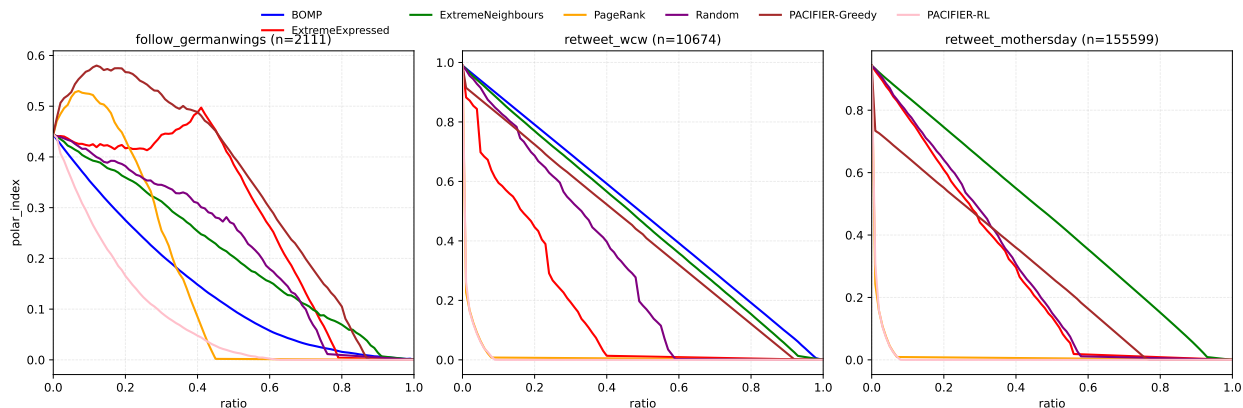


Figure 21: Real datasets (node_removal): representative polarization trajectories on three datasets (lower and earlier is better). Full trajectories are deferred to the Appendix.

interaction effects are critical: the benefit of one intervention depends heavily on subsequent equilibrium shifts, which cannot be captured by immediate reward regression alone.

The representative trajectories (Fig. 20) further illustrate this behavior. On small graphs, RL reduces polarization substantially earlier and maintains the lowest trajectory throughout the horizon. On medium and large graphs, RL continues to dominate both PageRank and BOMP, while Greedy often diverges upward after early steps, reflecting poor long-term credit assignment.

Overall, ME-continuous represents a regime where long-horizon reinforcement learning is essential. Unlike MI-type settings, myopic estimation fails to capture the compounding effects of expressed-opinion interventions, while PACIFIER-RL consistently exploits these dynamics across all graph sizes.

node_removal. When intervention alters the topology directly (node removal), the performance gap between long-horizon reinforcement learning and myopic estimation becomes even more pronounced. From the per-dataset AUC bars (Fig. 15), **PACIFIER-RL** achieves the best overall performance (avg. 0.027), substantially outperforming all classical baselines, with PageRank being the strongest non-PACIFIER competitor (avg. 0.037). In contrast, **PACIFIER-Greedy** performs poorly (avg. 0.186) and is highly unstable across datasets.

Per-dataset comparisons show that PACIFIER-RL wins on 14 out of 15 datasets (93% win rate), with an average relative improvement of approximately 19%. These gains are consistent across all scale buckets: 75% win rate on small graphs and 100% win rate on both mid- and large-scale graphs. By contrast, PACIFIER-Greedy wins on only one dataset, and often exhibits severe degradation relative to the best baseline, particularly on mid- and large-scale networks.

The heatmap (Fig. 17b) confirms that RL’s advantage is broadly distributed rather than driven by isolated datasets. Topology-altering intervention fundamentally changes future feasible actions and network connectivity patterns, making sequential credit assignment crucial. Without modeling long-term consequences, Greedy decisions frequently remove structurally suboptimal nodes, leading to cascading inefficiencies.

The representative trajectory plots (Fig. 21) further illustrate this behavior. Across small, medium, and large datasets, PACIFIER-RL consistently reduces polarization earlier and maintains the lowest trajectory throughout the intervention horizon. In contrast, PACIFIER-Greedy often diverges rapidly, reflecting the compounding cost of locally optimal but globally suboptimal removals.

Overall, node_removal represents the most sequentially complex regime among the extended settings. Here, long-horizon reinforcement learning is clearly essential, while myopic estimation fails to generalize under evolving topology.

6 Conclusion

We presented **PACIFIER**, a graph reinforcement learning framework for pacing opinion polarization dynamics via sequential network interventions. PACIFIER formulates the canonical MODERATEINTERNAL and MODERATEEXPRESSED problems as sequential decision-making tasks on networked opinion dynamics, enabling adaptive and scalable moderation without relying on handcrafted, model-specific heuristics. Within a unified framework, PACIFIER further

supports multiple FJ-consistent settings, including continuous-valued internal opinions, biased assimilation dynamics, and node removal. Empirical results on real-world Twitter follow and retweet networks demonstrate that PACIFIER consistently matches or outperforms strong baselines across datasets and intervention tasks.

This manuscript is an *arXiv preprint* intended to present the core framework and initial empirical evidence. In future revisions, we plan to expand the experimental suite, strengthen the analysis of generalization and robustness, and include additional ablations and comparisons to further clarify the strengths and limitations of the proposed approach.

Acknowledgments

This was supported in part by.....

References

- [1] Antonis Matakos, Evimaria Terzi, and Panayiotis Tsaparas. Measuring and moderating opinion polarization in social networks. *Data Mining and Knowledge Discovery*, 31(5):1480–1505, 2017.
- [2] Noah E Friedkin and Eugene C Johnsen. Social influence and opinions. *Journal of Mathematical Sociology*, 15(3-4):193–206, 1990.
- [3] Mohammed Lalou, Mohammed Amin Tahraoui, and Hamamache Kheddouci. The critical node detection problem in networks: a survey. *Computer Science Review*, 28:92–117, 2018.
- [4] Changjun Fan, Li Zeng, Yizhou Sun, and Yang-Yu Liu. Finding key players in complex networks through deep reinforcement learning. *Nature Machine Intelligence*, 2(6):317–324, 2020.
- [5] Kiran Garimella, Gianmarco De Francisci Morales, Aristides Gionis, and Michael Mathioudakis. Reducing controversy by connecting opposing views. In *Proceedings of the Tenth ACM International Conference on Web Search and Data Mining (WSDM '17)*, 2017.
- [6] Yue Wu, Linjiao Li, Qiannan Yu, Jiaxin Gan, and Yi Zhang. Strategies for reducing polarization in social networks. *Chaos, Solitons & Fractals*, 167:113095, 2023.
- [7] Cameron Musco, Christopher Musco, and Charalampos E. Tsourakakis. Minimizing polarization and disagreement in social networks. In *Proceedings of the 2018 World Wide Web Conference (WWW '18)*, 2018.
- [8] Zhiyuan Tu, Jeffrey Chan, Xiuzhen Zhang, and Shazia Sadiq. Adversaries with limited information in the friedkin-johnsen model. In *Proceedings of the 29th ACM SIGKDD Conference on Knowledge Discovery and Data Mining (KDD '23)*, 2023.
- [9] Nicholas Mylonas and Thanassis Spyropoulos. Opinion depolarization in social networks with graph neural networks. *arXiv preprint arXiv:2412.09404*, 2024.
- [10] Ashwin Arulselvan, Clayton W Commander, Lily Elefteriadou, and Panos M Pardalos. Detecting critical nodes in sparse graphs. *Computers & Operations Research*, 36(7):2193–2200, 2009.
- [11] Alfredo Braunstein, Luca Dall’Asta, Guilhem Semerjian, and Lenka Zdeborová. Network dismantling. *Proceedings of the National Academy of Sciences*, 113(44):12368–12373, 2016.
- [12] Pranav Dandekar, Ashish Goel, and David T. Lee. Biased assimilation, homophily, and the dynamics of polarization. *Proceedings of the National Academy of Sciences*, 110(15):5791–5796, 2013.
- [13] Kiran Garimella, Gianmarco De Francisci Morales, Aristides Gionis, and Michael Mathioudakis. Quantifying controversy on social media. *ACM Transactions on Social Computing*, 1(1):3:1–3:27, 2018.